TRANSLATIONAL REGULATION OF KIDNEY INJURY MOLECULE-1 MRNA: PRESENCE OF AN INTERNAL RIBOSOMAL ENTRY SITE

by

Nehir Banaz

B.S., Physics, Boğaziçi University, 2010

Submitted to the Institute for Graduate Studies in
Science and Engineering in partial fulfillment of
the requirements for the degree of
Master of Science

Graduate Program in Molecular Biology and Genetics

Boğaziçi University

2014

ACKNOWLEDGEMENTS

I am very grateful to my thesis supervisor İbrahim Yaman for his mentorship and guidance during my master's studies. He has trusted and accepted a physicist into his laboratory and raised me as a molecular biologist. He was always there for me where I had personal or work related problems and taught with patience, I learned a lot from him. I hope I will become a succesful scientist in the future and make him proud. I would also like to thank his wife Müge Çomar Yaman for reaching out to me during my mother's illness, her words brought me comfort and I am ever grateful for her sincere kindness.

I would like to thank my jury members Assist. Prof. Necla Birgül İyison and Prof. Arzu Karabay Korkmaz for accepting to be in my jury and spending their valuable time evaluating my thesis.

I am very grateful to my laboratory colleagues, they were a joy to work with and I am very lucky to have them as my lab mates. Zeynep Özcan taught me many of the cell culture techniques that I know and I consider her as an honorary big sister. She is a very compassionate person and I hope she will always be a part of my life. Gizem Gül and Hilal Kahraman never failed to make me laugh when I needed to laugh the most, they helped me with my work and they were wonderful friends. Tijen Bergin and Ayşin Demirkol were my project colleagues and together we attempted to solve the mystery of our beloved gene KIM-1. It was wonderful to have such good friends to rant with when experiments did not go the way we wanted.

I would also like to thank my friends and teachers at the MBG Department. I am not going to attempt to list their names because as usual I will forget some of them. These three years have been the worst and the best for me and thank you for creating an understanding and loving environment.

I also acknowledge financial support from the Turkish Scientific and Technological

Research Council (TÜBİTAK) through grant 110T919.

I could not have written this thesis without the help of two people, my mother and Kerem Uzel. I owe my mother not only my existence but also my interest in sciences and my will to finish what I have started. If she did not selflessly encouraged me to stay in the lab and get my master's degree when she was battling a terminal illness, I may have not succeeded in completing it. I know she would have been proud and I wish she was here to see me graduate. I thank Kerem not only for all the coffee he made and all the times he forced me to sit in front of the computer to write this thesis but also for his endless support. I am very lucky to have a boyfriend/flatmate who is also a colleague so I can discuss my research with him and ask for his help when I am stuck. He was by my side during my mother's illness and comforted me when she passed away. I owe most of my sanity to him, I am ever grateful and I believe we have the best in our future.

Finally, I would like to thank my life long friends Tuğba Büyükbeşe, Betül Kapıcıoğlu, Mirabella Güler Ağalar, Hülya Mete, Deniz Öztürk and Deniz Kıran. I am so lucky to have met all of you and I feel the need to acknowledge you in every work I create because you are a big part of who I am. Thank you for being such wonderful friends.

ABSTRACT

TRANSLATIONAL REGULATION OF KIDNEY INJURY MOLECULE-1 MRNA: PRESENCE OF AN INTERNAL RIBOSOMAL ENTRY SITE

Kidney Injury Molecule-1 (KIM-1) is a type I transmembrane glycoprotein that is highly upregulated on regenerating dedifferentiated renal proximal tubular epithelial cells as a consequence of toxic or ischemic injury. KIM-1 is a recognized biomarker of nephrotoxicity by United States Food and Drug Administration (FDA) and Europe Medicines Agency; therefore, understanding its transcriptional and translational regulation under chemotoxic stress is of the utmost importance. As chemotoxic stress inducers we used three xenobiotics, Ochratoxin A (OTA), Gentamicin (GM) and Cisplatin (CP) which are known to cause damage to kidney cells. The effects of these three xenobiotics on viability, proliferation, necrosis and apoptosis are examined using the immortilized human proximal tubule epithelial HK-2 cell line. The transcriptional start region of *Kim-1* gene is determined by Rapid Amplification of cDNA Ends (RACE). The changes in KIM-1 mRNA and protein levels are measured by Quantitative Real Time PCR and Western Blotting, respectively. Although there was a significant decrease in global protein synthesis upon xenobiotic treatment, KIM-1 protein levels increased. Furthermore, no significant change in KIM-1 mRNA levels can be detected which led us to suspect the existence of a possible post-transcriptional regulatory mechanism by which KIM-1 mRNA is translated via an Internal Ribosome Entry Site (IRES). This hypothesis is tested *in vitro* using bicistronic reporter vector pRF containing the 5'UTR of *Kim-1* gene. Our results confirm our hypothesis of a possible IRES localized around 300 bp upstream of the translation initiation codon.

ÖZET

BÖBREK HASARI MOLEKÜLÜ-1 MRNASININ TRANSLASYONEL DÜZENLENMESİ: DAHİLİ RİBOZOM GİRİŞ BÖLGESİNİN MEVCUDİYETİ

Böbrek Hasarı Molekülü-1 (KIM-1) toksik veya iskemik hasar sonrası dediferansiye olmuş böbrek proksimal tübül epitel hücrelerinde büyük ölçüde ifade edilen birinci tip transmembran bir glikoproteindir. KIM-1, Amerikan Gıda ve İlaç Örgütü (FDA) ile Avrupa İlaç Örgütü tarafından kabul edilmiş bir nefrotoksisite belirtecidir, dolayısıyla bu genin kemotoksik stres altında transkripsiyonel ve translasyonel düzenlenmesini anlamak oldukça önem arz etmektedir. Kemotoksisite ajanları olarak böbrek hücrelerinde stres yarattığı bilinen Okratoksin A, Sisplatin ve Gentamisin kullanılmıştır. Bu kimyasalların zaman ve doza bağımlı olarak insan böbrek hücre dizini HK-2 hücrelerindeki sitotoksik, nekrotik, apoptotik ve proliferatif etkileri saptanmıştır. cDNA Uçlarının Seri Amplifikasyonu (RACE) protokolüyle *Kim-1* geninin transkripsiyon başlangıç bölgesi belirlenmiştir. Ayrıca, kemotoksik ajanlar etkisinde KIM-1 mRNA ve protein ifadelerindeki değişimler kantitatif gerçek zamanlı polimeraz zincir reaksiyonu ve western blotlama teknikleri ile ölçülmüştür. Kimyasalla muamele sonrasında hücrelerdeki toplam protein sentezindeki azalmaya rağmen, KIM-1 geninin protein ifadesinin arttığı gözlemlenmiştir. Bunun yanı sıra, KIM-1 mRNA düzeyinde kaydadeğer bir değişim görülememiştir. Bu sebepten ötürü Kim1- mRNA'sının translasyonunun dahili ribozom giriş bölgesi (IRES) mekanizmasıyla post-transkripsiyonel olarak düzenlendiğine dair bir hipotez geliştirilmiştir. Bu hipotez *in vitro* ortamda iki raportör protein ve KIM-1 geninin 5'UTR bölgesini içeren pRF vektör sistemi kullanılarak sınanmıştır. Elde ettiğimiz sonuçlar olası bir IRES bölgesinin KIM-1 mRNA'sının translasyonel başlangıç kodonunun 300 baz yukarısında olduğunu destekler niteliktedir.

TABLE OF CONTENTS

LIST OF FIGURES

LIST OF TABLES

LIST OF ACRONYMS/ABBREVIATIONS

BrdU	5-bromo-2'-deoxyuridine
BUN	Blood Urea Nitrogen
cDNA	Complementary DNA
CIP	Calf Intestine Alkaline Phosphatase
CO_2	Carbon dioxide
CP	Cisplatin
ddH_2O	Double distilled water
DEPC	Diethyl-pyrocarbonate
dH_2O	Distilled water
DMEM	Dulbecco's modified Eagle's medium
DNA	Deoxyribonucleicacid
FBS	Fetal Bovine Serum
FDA	Food and Drug Administration
GM	Gentamicin
HAVCR- 1	Hepatitis A Virus Cellular Receptor-1
hKIM-1	Human KIM-1
hMADCAM-1	Human Mucosal Addressin Cell Adhesion Molecule-1
IRES	Internal Ribosome Entry Site
KIM-1	Kidney Injury Molecule-1
MMP	Matrix Metalloproteinase
NaCl	Sodium Chloride
OTA	Ochratoxin A
PCR	Polymerase Chain Reaction
PMA	Phorbol 12-myristate 13-acetate
PS	Phosphatidylserine
PTEC	Proximal Tubular Epithelial Cells
RDA	Representational Difference Analysis
RNA	Ribonucleicacid

rpm	Rotations per minute
RT	Room temperature
SDS-PAGE	SDS-Polyacrylamide Gel Electrophoresis
TBS	Tris-buffered saline
TBS-T	Tris Buffered Saline Tween
TIM-1	T-cell Immunoglobulin Mucin-1
tRNA	Transfer RNA
XTT	2,3-bis-(2-methoxy-4-nitro-5-sulfophenyl)-2H-tetrazolium-5-carboxanilide

LIST OF SYMBOLS

°C	Centigrade degree
g	Gram
hrs	Hours
kDa	Kilodalton
L	Liter
mg	Milligram
min	Minute
ml	Mililiter
mM	Milimolar
ng	Nanogram
rpm	Revolutions per minute
V	Volt
μg	Microgram
μl	Microliter
μM	Micromolar
κ	Kappa

1. INTRODUCTION

Kidney Injury Molecule 1 (KIM-1) is a type I transmembrane glycoprotein that contains a novel six-cysteine immunoglobulin-like domain and a mucin domain. Its expression is highly upregulated on regenerating dedifferentiated renal proximal tubular epithelial cells (PTEC) as a consequence of toxic or ischemic injury [1].

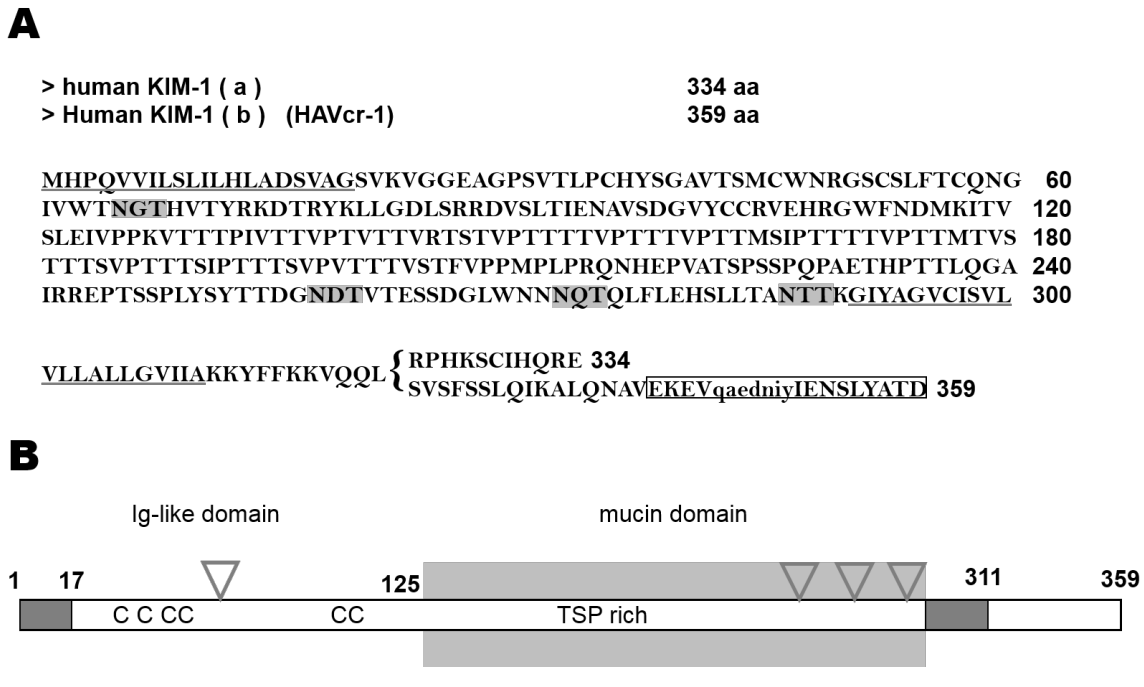

Figure 1.1. Amino acid sequence and the structural domains of human KIM-1 protein. (A) Sequences of two hKIM-1 variants a and b differing in their cytoplasmic domains. (B) Schematic representation of the hKIM-1b.

Structurally, KIM-1 belongs to the immunoglobulin gene superfamily. Since immunoglobulin-like domains have been implicated in cell-cell and cell-extracellular matrix interactions at the cell surface [1] and considering highly conserved structural homology of KIM-1 to several known adhesion molecules, such as mucosal addressin cell adhesion molecule 1 (MAdCAM-1), it may have a possible role in cell adhesion. In addition, the presence of several tyrosine kinase phosphorylation cites in the rela-

tively short cytoplasmic domain of KIM-1 suggests that KIM-1 may act as a signaling molecule [2].

Kim-1 is located on chromosome 5q33.2 and it codes for an mRNA with multiple splice variants. Two splice variants named KIM-1a and KIM-1b encode for two proteins that have identical extracellular domains and different cytoplasmic domains which show differential expression. KIM-1b transcript is predominantly expressed in adult kidney and it encodes a 359 amino acids long polypeptide whereas KIM-1a is expressed in liver and encodes a 334 amino acids long polypeptide [1].

KIM-1 has four N-glycosylation motifs that are shaded in gray in 1.1 A and multiple O-glycosylation sites. Three of these glycosylation motifs reside in the mucin domain whereas the first one resides in the Ig-like domain. It has been shown that the mature form of hKIM-1 that is sent to the membrane is approximately 100 kDA by cell surface biotinylation assays [1].

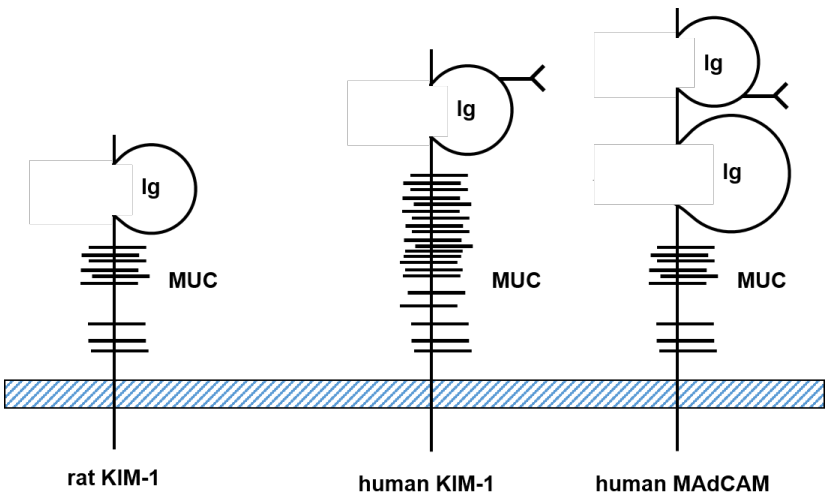

Figure 1.2. Structural domains of several KIM-1 proteins.

First KIM-1 orthologue was identified in African green monkey as hepatitis A virus cellular receptor-1 (HAVcr- 1) which is the receptor exploited by hepatitis A for viral entry in 1996 [3]. Two years later it was identified in rat by representational difference analysis (RDA) as a gene that responds to injury; thus, it is named as Kidney

Injury Molecule 1 (Kim-1) [2]. In 2002, human KIM-1 and its tissue distributions were described [1] and finally it was identified as T-cell immunoglobulin mucin-1 (TIM-1) in 2005 [4]. TIM-1 is expressed at low levels by subpopulations of active T-cells and the human orthologue of HAVcr- 1 (annotated as HAVCR-1) is expressed by hepatocytes [5].

The sequence of rat Kim-1 contains an open reading frame of 307 amino acids. Human and rat KIM-1 proteins are 43.8 % identical and 59.1 % similiar. Similarity between rat KIM-1 and monkey HAVcr-1 is 59.8 % over their entire amino acid sequences. Similarity between human KIM-1 cDNA and monkey HAVcr-1 cDNA is 85.3% [2]. Structural domains of several KIM-1 proteins are depicted in Figure 1.2.

1.1. Morphological Changes Occurring in the Proximal Tubules During Injury

In many acute and chronic diseases of renal origin epithelial cell injury occurs due to the toxin-rich supply of blood to the tubules. After such an injury tissue architecture should be remodeled similar to what happens during embryonic development. When a proximal tubular epithelial cell undergoes injury some of the following morphologic characteristics are observed that are illustrated in Figure 1.3 [6]:

(i) Loss of proximal tubular brush border
(ii) Loss of cellular polarity
(iii) Dedifferentiation
(iv) Apoptosis

During injury and repair some of the viable and apoptotic cells as well as the debris from the necrotic cells are released into the tubule which may form casts that cause luminal obstruction [2]. Surviving cells spread over the basal membrane, proliferate and cover the denuded tissue by undergoing mitogenesis and finally redifferentiating to establish a normal functional epithelium [7]. It is also crucial to clear the apoptotic bodies and necrotic debris to restore a functional normal tissue.

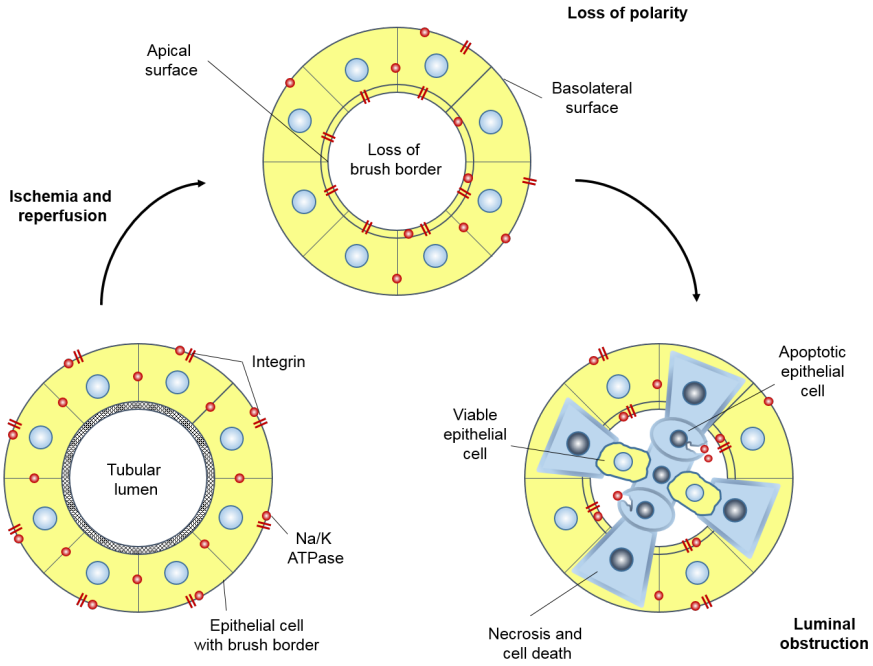

Figure 1.3. Tubular changes in the kidney during acute tubular necrosis.

1.2. KIM-1 Ectodomain Shedding

KIM-1 expression is detectable by western blotting using both a monoclonal antibody raised against the mucin domain of KIM-1 (ABE3) and a polyclonal antibody raised against the C-terminus in HK-2 and 769-P human kidney cell lines; an immortalized proximal tubular epithelial cell line and a kidney carcinoma cell line respectively [1].

When the conditioned media from the cells were collected and analyzed by western blotting, a protein that is 10 kDA smaller than the mature form of KIM-1 was detected and shown to be the soluble form of KIM-1 protein [8]. The membrane-bound form of KIM-1 protein run as 104 kDA whereas the soluble form is 90kDA [7].

KIM-1 ectodomain is shed into the urine from the injured proximal tubular epithelial cells and can be used as a biomarker for kidney disease. Using a human renal cell adenocarcinoma cell line 769-P, Bailly *et al.* demonstrated that KIM-1 shedding is

inhibited in the presence of two Matrix Metalloprotease (MMP) inhibitors BB-94 and GM6001. Also phorbol 12-myristate 13-acetate (PMA), a general activator of metalloproteinases, enhances shedding of KIM-1 by two-fold suggesting that KIM-1 shedding is mediated by matrix metalloproteinases [1].

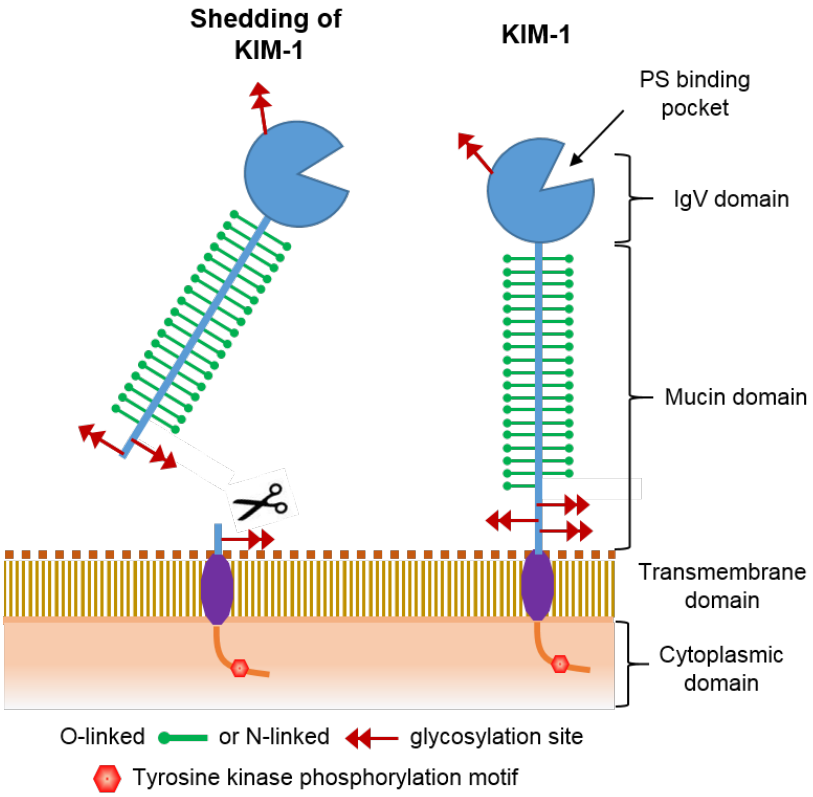

Figure 1.4. Representation of KIM-1 shedding.

In another study using the same cell culture system, pervanadate, a potent inhibitor of protein tyrosine phosphatases has been shown to enhance ectodomain shedding [9]. There is a rapid increase of KIM-1 shedding after pervanadate treatment and pretreating the cells with cycloheximide, a protein synthesis inhibitor, has no effect on pervanadate-induced KIM-1 shedding; suggesting that this effect is not dependent on active translation process. It can be speculated that pervadanate mimics physiologic stimuli such as growth factors. Both pervanadate induced and constitutive KIM-1 shedding is inhibited by metalloproteinase inhibitors thus both accelerated and constitutive shedding of KIM-1 is regulated by MMPs.

Pervanadate treatment has also rapidly increased activation of p-38 mitogen-activated kinases (MAPKs) and extracellular signal regulated kinase (ERK). By mutagenesis studies it is demonstrated that juxtamembrane secondary structure but not the primary amino acid sequence is important for KIM-1 cleavage. It is also demonstrated that the helical structure in the juxtamembrane section is to be maintained for metalloproteinaise cleavage probably for KIM-1 recognition and metalloproteinase accessibility [9].

1.3. KIM-1 Expression Under Stress Conditions

1.3.1. KIM-1 expression in post-ischemic kidney

Blood urea nitrogen (BUN) and serum creatinine are the conventional markers to assess renal function but they were proven ineffective in acute cases where nephrotoxicity occurs rapidly while it takes a lot longer for these markers to increase to reach to a sufficient level to be detected [10]. For many years a simple, sensitive and easily quantifiable marker has been needed and in 1998 during a research to identify genes that take role in injury and repair of the tubular epithelium, Kim-1 was found to be drastically upregulated in post-ischemic rat kidney by representational difference analysis (RDA) [2].

Although KIM-1 is basally expressed in certain immortalized or cancer cell lines, it is not expressed in normal kidney of animal models or humans, this fact insinuates KIM-1's function as a sensitive biomarker for kidney injury. Northern blot analysis indicates that Kim-1 mRNA is expressed at low levels in control and embryonic kidneys but dramatically up-regulated in 48-hour postischemic rat kidney. These findings are confirmed by western blotting using antibodies directed against the cytoplasmic domain of KIM-1 or a fusion protein of glutathione S-transferase (GST) linked to the NH2-terminal Ig domain of the rat KIM-1 protein [2].

Han *et al.* published the first study showing a drastic increase of KIM-1 expression in human kidneys with acute tubular necrosis (ATN); thus, proving KIM-1's value as

a strong biomarker for humans with kidney injury [8]. The authors quantified KIM-1 levels in the urine of patients with several forms of kidney injury by using western blotting and revealed that very high levels of soluble KIM-1 were present in the urine of patients with ischemic ATN [8].

As KIM-1 was shown to form a sensitive urine marker for proximal tubule injury [8], another report indicated that a cleaved form of KIM-1 is present in the culture media of human renal tumor cell lines [1]. As a result, KIM-1 is hypothesized to form an ideal candidate as a biomarker for renal cell carcinoma (RCC). Indeed, a recent study that investigated tissue and urine samples from patients with RCC and nonrenal tumors found out that KIM-1 expression is very specific for tumors of renal origin, urinary KIM-1 is highly abundant in patients with renal primary tumors of all stages, KIM-1 is present in lymph nodes to which the tumor has metastasized and a strong correlation between the size of a renal tumor and urinary KIM-1 levels is available [11]. Thus, apart from its association with acute renal failure, KIM-1 is also proposed to serve as a screening marker for renal tumors.

KIM-1 is in the list of recognized biomarkers of nephrotoxicity by United States Food and Drug Administration (FDA) and Europe Medicines Agency [12]. Research groups have developed ELISA tests to quantify KIM-1 presence in the urine to assess renal injury in rat and many clinical trials are being conducted for humans [10].

1.3.2. Expression of KIM-1 mRNA and Protein Levels *in vitro*

Since KIM-1 was identified as a sensitive biomarker for ischemia, it is important to determine if KIM-1 mRNA and protein levels are upregulated under chemotoxic stress and subsequently to assess whether KIM-1 can be used as a general nephrotoxicity biomarker. There are several studies assessing KIM-1 mRNA and protein levels in various cell types and under diverse xenobiotics.

Khandrika *et al.* performed a study using oxalate, a metabolic end product excreted by the kidney, as a stress inducer which resulted in increased KIM-1 mRNA

and protein levels in HK-2 cells [13]. In the same study, the authors further developed a murine *in vivo* model for hyper-oxaluria and determined elevated levels of KIM-1 mRNA compared to normal controls using RT-PCR. They confirmed their findings by western blotting showing an increase in protein levels as well. In addition to increased KIM-1 expression both in mRNA and protein levels, they also noted increased levels of KIM-1 shedding in urine collected from hyperoxaluric rats [13].

Mukherjea *et al.* performed a study to assess differential expression of KIM-1 due to cisplatin toxicity in rat cochlea and in three different mouse transformed cell lines [14]. They were able to demonstrate that KIM-1 mRNA expression level increases in the rat cochlea after cisplatin administration and observed hearing loss. When rats were pretreated with lipoic acid which is a scavenger of reactive oxygen species the cisplatin induced hearing loss together with KIM-1 mRNA expression decreased. As they have used primers derived from the rat and mouse kidney cDNA and were still able to detect KIM-1 in rat cochlea, it can be suggested that the KIM-1 mRNA in the cochlea is similiar in sequence to what is observed in the kidney [14].

1.4. Functions of KIM-1

As professional phagocytes macrophages would be the first candidates to perform clearance in the injured tubular epithelium where they are rarely seen. When they are present they are not localized inside the tubule but in the interstitium. In addition to macrophages, neighboring epithelial cells are also postulated to contribute to this process [5].

Based on their studies, Ichimura *et al.* postulated that KIM-1 takes over the role of macrophages in tubular clearance by turning epithelial cells into phagocytes [5]. They have shown internalization of apoptotic bodies within KIM-1 expressing epithelial cells at injured rat kidney tubules using confocal microscopy *in vivo*. Furthermore, in all of the rat, porcine and canine kidney primary epithelial cell lines KIM-1 and apoptotic bodies were colocalized, where KIM-1 positive phagocytic cups were seen to engulf apoptotic bodies. Many apoptotic thymocytes were localized in KIM-1 expressing ep-

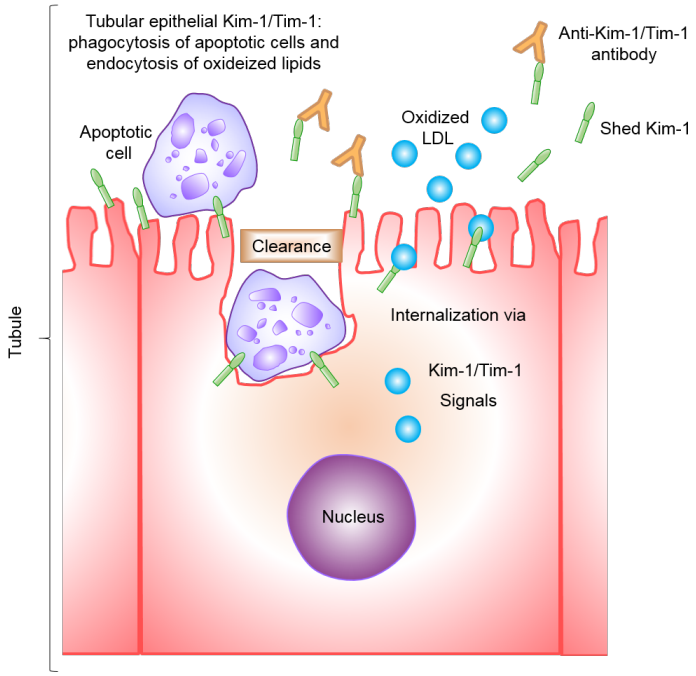

Figure 1.5. Functions of KIM-1 in clearence of oxidized LDL and phagocytosis of cell debris.

ithelial cells when co-cultured. Flow cytometric analysis measured 10-fold increased florescence in stably KIM-1 expressing porcine renal tubular cells compared to the control. The authors also observed that stably KIM-1 expressing cells ingested necrotic cell debris 15 times more than the control cells, confirming that the KIM-1 expressing epithelial cells can internalize both apoptotic bodies and necrotic debris. Serum derived opsonins are known to help phagocytes such as macrophages but there were no difference in KIM-1 mediated phagocytosis in the absence or presence of serum. It is demonstrated that KIM-1 ectodomain specifically binds to phosphatidylserine (PS) and oxidized low-density lipoprotein (LDL) as well as some gram-negative and gram-positive bacterial cell surface epitopes but not to the yeast cell wall [5].

It is known that removal of the casts obscuring the tubule in a timely fashion is fundamental not only for restoration of function but also for the prevention of inflammatory immune response and that phagocytosis leads to production of anti-inflammatory cytokines. A multi-functional cytokine, hepatocyte growth factor (HGF) is released

by mesenchymal cells and also plays an important role in renal repair. Overexpression of KIM-1 in porcine renal tubular cells (KIM1-PK1) increased the HGF mRNA expression [5] suggesting a possible role for KIM-1 in the renal regenarative mechanism. KIM-1 colocalizes with markers of proliferation (BrdU) and dedifferentiation (vimentin) as well which also insinuates a possible role for KIM-1 in the regeneration process [2]. Bailly *et al.* have shown that recombinant KIM-1 expression results in an altered cell motility and scattering, indicating that KIM-1 could be involved in the migration of the dedifferentiated cells, facilitating the reconstitution of a continuous epithelial layer [1].

It is still not clear how KIM-1 triggers internalization of phagocytosed material but the tyrosine phosphorylation sites in its cytoplasmic tail are good candidates to initiate an intercellular signaliging cascade. Overall, current data suggest that renal tubular epithelial cells undergo epithelial–mesenchymal transition after serious injury during which they increase the expression of KIM-1 working as a scavenger protein. In addition, KIM-1 may possibly take a role in HGF secretion and confering motility to cells during remodelling of the epithelial tissue.

1.4.1. Function of KIM-1 in the Immune System

KIM-1 is also identified as T cell immunoglobulin domain and mucin domain-containing protein 1 (TIM-1) because it has been reported to be expressed on immune cells to varying degrees [15]. Tim-1 is associated with a high risk of developing asthma and it has been genetically linked to Th2-driven murine airway hypersensitivity [16]. It has also been proposed to be an activating receptor in multiple cells functioning in the immune system such as T cells, B cells and dendritic cells [17]. However Ichimura *et al.* criticizes many papers published on KIM-1/TIM-1 based on the antibody selections and on several other accounts and suggests that antibody blocking experiments should be done with a standardized antibody that has a high specificity to TIM-1/KIM-1 [15].

1.5. Xenobiotics Used in This Study

1.5.1. Ochratoxin A (OTA)

Ochratoxin A (OTA) is a mycotoxin, secondary metabolite of fungal species, and it is produced by genera *Penicilium* and *Aspergillus* [18]. OTA contaminates a wide variety of cereal and agricultural products as well as spices, wine, beer, coffee, nuts and chocolate which means that the daily rate of OTA exposure for humans is very high [19]. OTA is a derivative of phenylalanine-dihydroisocoumarine and its resemblance to this amino acid is thought to cause inhibition of protein synthesis by binding to phenylalanine tRNA synthetase [20].

International Agency for Research on Cancer classified OTA as a possible human carcinogen due to the sufficient experimental evidence for carcinogenicity in animal studies [21]. The target organ of OTA is kidneys and it is considered as a potent renal carcinogen in rats, mice and humans [22]. However, OTA is not a direct genotoxic carcinogen and it is thought that OTA's genotoxic effects occur through secondary mechanisms such as oxidative stress [18]. It is suggested that OTA might produce single-strand DNA breaks and oxidative DNA damage in the human renal proximal tubular epithelial cell line (HK-2) but the mechanism by which OTA contributes to nephrotoxicity, is not known [23]. In humans, OTA is also related to Balkan endemic nephropathy [24].

1.5.2. Gentamicin (GM)

Gentamicin (GM), an aminoglycoside antibiotic, is a powerful xenobiotic which interrupts protein synthesis through binding to the 30S subunit of the bacterial ribosome [25]. It originates from the genus of a gram-positive bacteria *Micromonospora* while being particularly effective against gram-negative bacteria [25].

Similar to other aminoglycoside antibiotics, gentamicin is also reported to be ototoxic and nephrotoxic [26]. Its nephrotoxic impact is more frequently reported [27]

and forms a therapeutical limitation [28]. Although the main contribution of aminoglycoside nephrotoxicity is known to be tubular damage [28], the exact mechanism of gentamicin's nephrotoxic effect is not fully understood. Nevertheless, it is reported that gentamicin leads to tubular, glomerular and vascular effects [28]. Additionally, gentamicin results in phospholipidosis which also contributes to nephrotoxicity [29].

1.5.3. Cisplatin (CP)

Cisplatin (CP) is an anti-cancer drug that causes crosslinking of DNA which leads to programmed cell death in dividing cells [30]. Since xenobiotics are filtered by the glomerular structures located in kidney in order to be excreted, they are found in much more concentrated values in kidney compared with other parts of the organism. Thus, CP concentration piles up in distal and proximal nephrons of the proximal tubule in kidney and this accumulation generates a nephrotoxic impact [31].

The neprotoxicity is developed through conjugation of the cation transporter to glutathione and its metabolization into a reactive thiol in proximal tubules [32]. Cisplatin is reported to activate three MAP kinases in kidney tissue *in vitro* and *in vivo*, thus MAPK signaling pathway is assumed to be interfered at cisplatin's nephrotoxic impact [33]. Additionally, nephrotoxicity due to cisplatin accumulation is though to be associated with hypoxia and mitochondrial injury. Finally, KIM-1 gene is also reported to be drastically upregulated during cisplatin treatment [34].

1.6. Translational Regulation of Gene Expression Under Cellular Stress Conditions

In their life span, cells encounter and must defend against several stressful conditions such as nutrient stress, DNA damage, hypoxia, Endoplasmic Reticulum (ER) stress and temperature shock which they respond by changing expression of their protein repertoire. This change can be achieved by shutting down the general protein synthesis and specifically producing proteins that respond to stress stimuli. Gene expression is mostly regulated at the translational level. It allows immediate changes in

protein expression, providing the cells the necessary plasticity for responding to the rapid changes of environmental conditions. There are many studies reporting a lack of correlation between mRNA and protein levels of several genes employed in stress response by comparing the genomic and proteomic profiles of cells [35]. This fact indicates the importance of post-transcriptional control of gene expression.

1.7. Two Different Mechanisms for Eukaryotic Translation Initiation

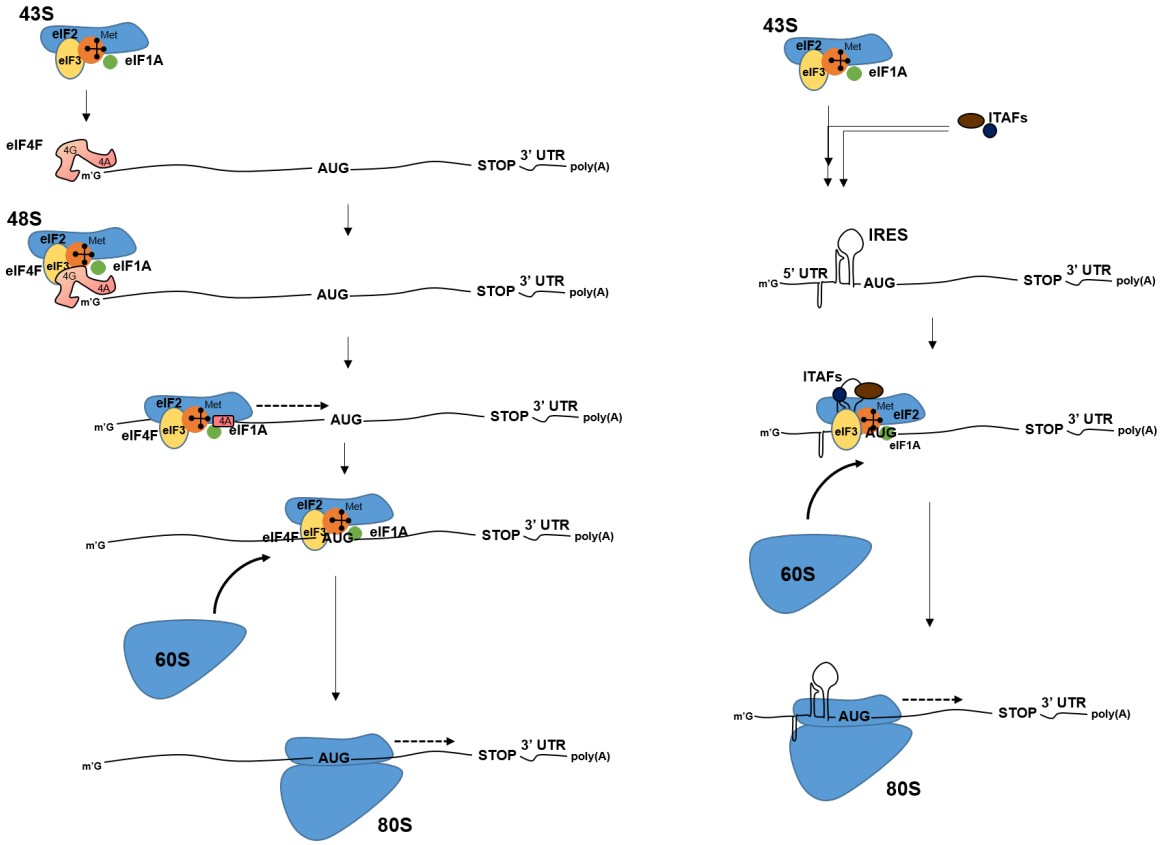

Figure 1.6. Different mechanisms for translation initiation.

Translation of a protein is usually controlled at the initiation level, because it is harder to stop later and an unfinished protein product may have harmful effects on the cell [36]. The conventional initiation mechanism involves sequential binding of 40S and 60S ribosomal subunits to a messenger RNA, respectively. This way of initiating protein synthesis involves cap-dependent scanning in which eIF4F protein complex

(encompassing eIF4E, eIF4G and eIF4A) fastens on the 5' m7G cap structure on the mature mRNA and recruits the 40S ribosomal subunit by interacting with eIF3 that is tethered to 40S [37] and forming the 43S ribosomal complex. By using many initiation factors regulating the binding of 40S to mRNA, the cell is capable of controlling the overall rate of translation as well as adjusting relative rates of expression for various types of messenger RNAs [38]. eIF2-GTP-Met-tRNA comes and tethering to the 40S ribosomal subunit complex in order to initiate translation once docking on an mRNA occurs [39]. This is easier said than done since scanning can be impeded by secondary structures in the mRNA which may form very stable hairpin loops that can not be unwinded by the 43S ribosomal complex thus obstructing its passage [38].

An alternative mechanism for translation initiation is utilization of an internal ribosome entry site, abreviated as IRES, which are structures in the 5' UTR of a mature mRNA that recruits the 43S ribosomal complex to recognize translational start codon without the scanning process. IRESs were first discovered in RNA viruses Hepatitis C virus and encephalomyocarditis virus (EMCV). Since these polioviruses lack a 5' G cap, it is appearant that they evolved a different way of initating translation. The secondary structure in the 5' untranslated region (5' UTR) of the mRNA acts as a docking ground for the ribosome. This mechanism has various advantages: Viruses can inhibit the normal translation mechanism in host cells which is G-cap dependent and still produce the viral proteins. In eukaryotic cells when the cap-dependent protein synthesis is compromised during stress conditions such as hypoxia, amino acid deficiency or apoptosis, the proteins that are needed to overcome this situation can be synthesised using the same principle. This is to be expected since under conditions that require such proteins the lag that is associated with the syntheis, processing and nuclear export of *de novo* synthesized mRNA may comprise cells ability to respond.

Although the existence of viral IRESs are well documented, accepted and many viral IRESs became commercially available molecular biological tools, our knowledge of cellular IRESs and their regulation is still evolving [35]. Cellular IRESs are mostly reported in mRNAs with long 5'UTRs and a high GC content which creates a very stable secondary structure that is hard for the ribosomal helicases to unwind [40].

However there are no consensus sequences or discernable features to indicate existence of an IRES which makes detection of an IRES reliant in empirical assays.

2. PURPOSE

The expression of KIM-1 is upregulated *in vivo* at mRNA and protein levels as a consequence of toxic or ischemic injury and it is a sensitive biomarker of nephrotoxicity recognized by United States Food and Drug Administration (FDA) and Europe Medicines Agency. Besides, knowing the critical role of KIM-1 in the clearance of apoptotic and necrotic cell debris from the injured site of the kidney, virtually no study exists intended to better understand the regulation of Kim-1 gene at the transcriptional and post-transcriptional levels. Thus, the aim of this project is the elucidation of KIM-1's transcriptional and translational regulation under chemotoxic stress. Initially, chemotoxic stress conditions were established in HK-2 cell line induced by three different xenobiotics: OTA, CP and GM. Their effects on cell viability, proliferation, necrosis and apoptosis were measured. Next, in order to better understand the transcriptional regulation of KIM-1, 5'RLM-RACE experiment was conducted for characterization of the transcription start region of *Kim-1* gene. Then, using the previously established cell culture and chemotoxic stress induction model, the expressions of KIM-1 RNA and protein upon treatment with xenobiotics were determined. After detecting an increase in KIM-1 protein levels while global protein synthesis is significantly decreasing and observing no significant change in KIM-1 mRNA, a post-transcriptional regulation mechanism through an internal ribosome entry site (IRES) was hypothesized. Finally, this hypothesis was tested *in vitro* in HK-2 cell line by utilizing bi-cistronic expression vectors and a possible IRES sequence was localized within the 5'UTR of KIM-1 mRNA.

3. MATERIALS AND METHODS

3.1. Materials

3.1.1. Cell Culture

HK-2 cells are procured from American Type Culture Collection (ATCC) and grown in 10% FBS, 100 U/ml penicillin, 100 μg/ml streptomycin in DMEM/ F:12 (Ham) (1:1) media at % 5 CO_2 and 37 °C.

3.1.2. Ochratoxin A (OTA), Cisplatin and Gentamicin for Treatment

OTA was purchased from SIGMA Medical Supplies Corp., dissolved in ethanol and kept as 10 mM stock solutions at −80 °C. Ethanol concentration is always kept at 0.1% during treatments and control groups were also treated with 0.1% ethanol. Cisplatin was purchased from Santa Cruz, dissolved in saline water and kept as 5 mM stock solutions at −80 °C. Gentamicin was purchased from Hyclone, dissolved in saline water and kept as 50 mg/ml stock solutions at −80 °C.

3.1.3. Equipment and Supplies

A list of equipment and supplies used can be found in Appendix A and B.

3.2. Methods

3.2.1. Thawing of Cells

HK-2 cells were retrieved from −150 °C freezer and immediately put on ice. Then the cells were melted at 37 °C in waterbath and transferred into 15 ml falcon tubes. Warm medium was slowly added to the cells which was followed by centrifugation at 300g for 5 minutes. Supernatant was discarded and the pelletwas resuspended in the

growth medium. Finally, the cells were plated into cell culture plates.

3.2.2. Maintanence of Cells

HK-2 cells were cultured in Dulbecco's Modified Eagle Medium F-12 (DMEM/F-12) supplemented with 10% fetal bovine serum (FBS), 100 U/ml penicillin, and 100μg/ml streptomycin. The cells were incubated in humidified incubator at 5% CO_2 and 37 °C.

When cells reach 70% confluency, they were washed with PBS and treated with 0.05% trypsin for 5 minutes at 37 °C. The cells were then transferred into 15 ml falcon tubes and centrifuged at 300g for 5 minutes. Following centrifugation the supernatant was discarded and the pellet was resuspended in the growth medium. Before a new experiment is started the cells were counted with a hemocytometer.

3.2.3. Storage and Freezing of Cells

Cells were grown until they cover the plate and washed with PBS. They were trypsinized for 5 min at 37 °C and then they were collected in a 15 ml falcon in growth medium. Cells were pelleted at 300g for 5 minutes. Supernatant was discarded and the pellet was resuspended in FBS. Dimethyl sulfoxide (DMSO) was added until it is 10% of the final volume. Finally cells were transferred into a cryovial and stored at −150 °C.

3.2.4. Transformation

After thawing 50 μl of competent cells on ice for 5 minutes, 10-50 ng plasmid DNA or 10 μl ligation reaction mix was added to the cells. The mixture was incubated on ice for 30 minutes which was followed by a heat-shock step in a waterbath at 42 °C for 90 seconds. After the heat shock step the mixture was transferred to ice and kept on ice for 5 minutes. Then as a recovery step, 500 μl of fresh LB was added to the cells and the mixture was incubated at 37 °C for 60 minutes. Finally, 100 μl of the transformation mixture was spread on appropriate selection plates.

3.2.5. Preparation of Competent Cells (Calcium Chloride Method)

First, a single colony of the DH5α bacteria strain was picked and inoculated overnight at 37 °C in 5 ml LB medium. 500 μl of the overnight culture was used to inoculate 500 ml of fresh LB medium and incubated at 37 °C on a shaker until the OD550 reached a reading of 0.6. Then the bacteria culture was chilled on ice for 15 minutes and centrifuged at 3000 rpm for 10 minutes at 4 °C. The supernatant was removed and bacteria were resuspended gently in the remaining supernatant. 500 μl of 50 mM CaCl2 solution was added and incubated on ice for 30 minutes. Another centrifugation step was performed at 3000 rpm for 10 minutes at 4 °C, the supernatant removed and 20 μl of 0.1M CaCl2 (with 15% glycerol) solution was added to resuspend the pellet. Finally the bacteria suspension was divided in 50 μl aliquots and immediately shock frozen in liquid nitrogen. Aliquots were stored in -80 °C until transformation.

3.2.6. Ligation

For ligation reactions, a 1:3 molar ratio of vector to insert was used. The relative intensities of vector and insert after gel electrophoresis, concentrations measured by Nanodrop Spectrophotometer and the size of the DNA fragments were used to estimate the amount of the DNA. Ligation reactions include vector and insert DNA (up to 100 ng), 1 μl of T4 DNA ligase (NEB), 2 μl of 10x Ligase Buffer and dH2O was added up to a final volume of 20 μl. The reaction mixture was incubated at 25 °C for 1 hour or overnight, followed by transformation into competent cells.

3.2.7. Restriction Digestions

Restriction digestions were performed with endonuclease enzymes from New England Biolabs, Promega or Fermentas. Reactions contain 1-5 units of restriction enzymes per microgram of DNA and 1X concentration of the buffer that was recommended and supplied by the manufacturer. If necessary 1X BSA was added to the reaction. Digestion reactions were incubated at 37 °C for 1 to 8 hours.

3.2.8. Agarose Gel Electrophoresis

DNA samples were run in 1% agarose gel containing ethidium bromide (0.5μg/ml) until DNA fragments were separated as desired. As a molecular weight marker 1kb DNA ladder (NEB, USA) was used. The visualization of agarose gels was performed under UV light. Finally they were documented as electronic TIF files.

3.2.9. DNA Extraction from the Gel

DNA fragments were extracted from agarose gels using the Roche High Purification kit and NucleoSpin Gel and PCR Clean-up kit (740609.50, Macherey-Nagel). Agarose gel blocks containing the DNA fragment of interest were cut out using a scalpel. Then 100 μl of binding buffer per 0.01g of agarose gel was added. The mixture was incubated at 56 °C for 10 minutes to allow the gel to dissolve in the buffer. Next, 50 μl of isopropanol per 0.01g of agarose gel was added and the mixture was loaded to spin columns provided with the kit, washed, and eluted using Tris/EDTA. Eluted DNA was quantified with NanoDrop Spectrometer and visualized on agarose gel.

3.2.10. PCR Purification

NucleoSpin Gel and PCR Clean-up Kit (740609.50, Macherey-Nagel) was used according to the manufacturer's instructions to purify PCR products and digested plasmid fragments.

3.2.11. Plasmid Isolation

Plasmid isolation was performed using the Plasmid MiniGeneJet Isolation kit (Thermo Scientific) and NucleoBond Xtra Midi Kit (740410.2, Macherey-Nagel) according to manufacturer's instructions.

3.2.12. Transfection of Plasmids

For transfection with dual luciferase constructs, three different wells were transfected with the same plasmid/construct. The transfection mixture for each triplicate contains 1 μg of plasmid DNA, 1.25 μl of X-treme GENE Transfection Reagent (Roche) and approximately 100 μl of transfection medium for each well. The mixture was incubated for one hour at room temperature before 100 μl of transfection mixture was added to each well. Finally 12-well plates were incubated for 24 hours at 37 °C before luciferase assays.

3.2.13. Lysis of Cells and Luciferase Assays

Lysis of cells was performed 24 hours after transfection and luciferase assays are performed with Dual-Luciferase Reporter Assay (Promega) with buffers provided by the manufacturer according to the instructions. The luminescence was measured in a 96-well plate reader (Thermo Scientific, Fluroskan Ascent Fl). The luminometer was set to dispense 100 μl firefly luciferase substrate, delay 2 seconds and measure luminescence for 1 second. After measurement, 100 μl Stop & Glo Reagent was added, incubated for 15 minutes and luminescence of renilla luciferase was measured for 1 second.

3.2.14. Total RNA Isolation

TRIpure (Invitrogen) protocol was performed to isolate total RNA from cells according to the manufacturer's instructions. HK-2 cells were grown in a monolayer covering 10 cm cell culture dishes. 24 hours after treatment medium was removed and 500 μls of TRIpure Isolation Reagent(Roche) was added to each plate. Cells were scraped by a plastic scraper for lysis. Lysates were pipetted several times in order to create a homogenized mixture and then transferred into 2 ml eppendorf tubes. Lysates were incubated at room temperature for 5 minutes before 100 μl chloroform was added to each tube. Tubes were shaken for 15 seconds to properly mix the solution and then incubated at room temperature for 5 minutes to allow for phase seperation.

Samples were then centrifuged at 12000g for 15 minutes at 4 °C until the solution was visibly separated into three phases. The aqueous phase was transferred into a new 1.5 ml tube and 250 μl of 100% isopropanol was added to the aqueous phase in order to precipitate the RNA. Samples were again incubated for 5 minutes at room temperature and centrifuged at 12000g for 10 minutes at 4 °C and the supernatants were discarded. 500 μls of 75% ethanol was added to the samples which are then vortexed and centrifuged at 7500 g for 5 minutes at 4 °C. The precipitated total RNA was resuspended in double distilled water treated with Diethyl-pyrocarbonate (DEPC).

3.2.15. RNA Ligase Mediated Rapid Amplification of cDNA Ends

For RLM-RACE, FirstChoice RLM-RACE Kit (Ambion) was used acording to the manufacturer's instructions. In order to eliminate the phosphate ends from 5' degraded mRNAs, rRNAs and tNAs, the protocol starts with treatment of 1 μg extracted total RNA of (HK-2 cells) with 2 μl of Calf Intestine Alkaline Phosphatase (CIP; Promega) for 60 minutes. After the removal of CIP via phenol:chloroform extraction, the solution was then treated with 1 μl of Tobacco Acid Pyrophosphatase (TAP) to remove m7G-Cap structures from full lenght mRNA molecules in the sample. Next, 5'RACE adapters were ligated to full length mRNAs using T4 RNA Ligase (Promega) and stored at -80 °C. 2 μls of this solution was used to synthesize first-strand RLM-RACE cDNA and subsequent PCR reactions were performed using the provided inner primer and the designed gene-specific primer. Finally, amplified PCR products were cloned to pGEM-T Easy (Promega) vector system for further sequence analysis.

3.2.16. XTT Cell Viability Test

Cell Proliferation Kit II (XTT) was purchased from Roche and used for determining viability of HK-2 cells that are grown in DMEM media. The assay is based on the cleavage of yellow colored tetrazolium salt XTT which turns into an orange formazan dye during metabolic activities of cells. The dehydrogenase enzymes in metabolically active cells perform the cleavage so this process only occurs in live cells. The resulting

orange formazan dye is soluble in water, so it is possible to directly quantify viability using a scanning multiwell spectrophotomer (ELISA reader).

HK-2 cells were seeded at a density of 5x10^3 cells/100μl per well on clear-walled 96-well tissue culture plates and treated with different concentrations of CP, GM and OTA for 24, 48 and 72 hours. After the designated treatment time, 50 μl of XTT labeling reagent was mixed with 1 μl of electron coupling reagent for each well and added to the treated cells without removing the media. Cells were incubated at 37 °C for 4 hours and absorbance was measured at 490 and 655 nm using an ELISA reader.

3.2.17. CytoTox-Glo Cytotoxicity Assay

CytoTox-Glo Cytotoxicity Assay was purchased from Promega and used to determine cell death by necrosis. The assay uses alanyl-alanyl- phenylalanyl-aminoluciferin, a luminogenic peptide substrate and measures the protease activity released by the cells that have died via necrosis thus lost their membrane integrity. The luminogenic peptide substrate can not cross the intact membrane of live cells so it can not generate signal from the live cell population. The luciferase is thermostable so it creates a stable luminescent signal which can be measured up to 4 hours without a significant loss in signal quality.

HK-2 cells were seeded at a density of 5x10^3 cells/100μl per well on white-walled 96-well tissue culture plates. The cells were treated with designated concentrations of CP, GM and OTA and incubated at 5% CO_2 and 37 °C for 24 hours. Cytotox-Glo reagent was prepared according to the manufacturer's instructions and added to both treated and control samples which were then shaked at an orbital plate shaker at room temperature for 15 minutes. The luminescence was measured in a 96-well plate reader (Thermo Scientific Fluroskan Ascent Fl). To measure total cell number 50 μl of lysis reagent was added to each well and the plate was shaked gently at room temperature for an additional 15 minutes. The luminescence was again measured in Thermo Scientific Fluroskan Ascent Fl.

3.2.18. Bromodioxyuridine (BrdU) Incorporation Assay

BrdU Incorporation Assay was purchased from Roche and used in order to assess proliferation rate which relies on 5-bromo-2'-deoxyuridine incorporation into DNA instead of thymidine during DNA replication. The incorporated BrdU was detected by BrdU immunoassay. HK-2 cells were seeded at a density of $5x10^3$ cells/100μl per well on 96-well plates with white bottoms. Cells were labeled with BrdU for 4 hours and media were removed. FixDenat solution was added and cells were incubated at room temperature for half an hour. Following incubation FixDenat was removed and anti-BrdU POD was added to the cells and incubated for an hour at room temperature. Following this the substrate was added and 10 minutes later the chemiluminescence was measured using a luminometer.

3.2.19. Western Blotting

3.2.19.1. Cell Lysis and Protein Extraction. Cells were cultured in 10 cm plates and washed with PBS before lysing with 400 μl RIPA buffer containing Phos-STOP phosphatase inhibitor cocktail and complete EDTA-free protease inhibitor cocktail (Roche). Following lysis cells were incubated for 5 minutes on ice and scrapped by a rubber policeman. Lysates were incubated on ice for 30 minutes and homogenized by passing through 25-gauge syringes several times. Finally, lysates were centrifuged at 14000 rpm for 15 minutes at 4 °C and the supernants were transferred into a new 1.5 ml eppendorf tube.

3.2.19.2. Quantification of Protein Lysates. Protein concentrations were measured by using BCA Protein Assay Kit (Pierce). Thermo Scientific 23210 solution was serially diluted in PBS to final concentrations of 0.125, 0.25, 0.5, 1 mg/ml to serve as standards. Protein samples were also diluted in PBS in 1 to 4 ratio. BCA working solution was prepared by mixing Reagent A and Reagent B in 1 to 50 ratio. To start with 1X PBS (blank standard), 10 μl of diluted proteins samples and BSA standards were added into 96-well plate and then 200 μl of BCA working solution was added. After this the 96

well plate was incubated at 37 °C for 30 min and the absorbance values were measured at 562 nm on the plate reader. Following this, blank measurements were subtracted from the measurements of BSA standards and the protein samples. Standard curve was obtained by using subtracted BSA standard measurements versus the concentrations. According to the standard curve the concentrations of protein samples were calculated.

3.2.19.3. Preparation of Protein Lysates. To prepare the protein lysates for loading on the gel, appropriate volumes of PBS and 4X protein loading buffer were added to the 20 μg of protein samples and the samples were boiled at 95 °C for 5 minutes.

3.2.19.4. SDS-Polyacrylamide Gel Electrophoresis (PAGE). 12% resolving and 5% stacking polyacrylamide gel solutions were prepared and poured between the glass plates. After polymerization, the samples were loaded on gel with 4 μl of Fermentas prestained marker and run in 1X SDS buffer at 100 V until the samples reach the resolving gel. Following this step, the voltage was increased to 120 volts and the samples were run until the bromophenol dye reach to the end of the gels. The separated proteins were transferred onto Polyvinylidene difluoride (PVDF) membrane (Millipore) with Bio-Rad wet transfer system.

The membrane and the Watmann papers were cut according to the size of the gel. The membrane was immersed in absolute methanol and in distilled water. The gel and membrane were sandwiched between Watmann papers and sponges. Transfer was done in 1X transfer buffer and the duration of the transfer was arranged according to protein sizes at 4 °C. Membranes were washed in TBS-T once for 5 minutes and they were incubated in blocking solution for an hour. After blocking the membranes were washed three times in TBS-T each for 5 minutes. Then the membranes were incubated in primary antibody solution at 4 °C overnight. The next day, the membranes were washed in TBS-T three times and they were incubated in secondary antibody solution for 1 hour at room temperature. After three more washing steps, the membranes were incubated in LumiGLO solution (Cell Signaling Technologies) for 1 min at room temperature and then the chemiluminescent signals were captured using Stella digital bioimaging

system (Raytest). The band intensities were analyzed using ImageJ software.

3.2.20. Statistical Analysis

Experiments were performed in triplicates and data was analyzed using GraphPad Prism v5.04. Errors were calculated as mean ± SEM and the significance was tested by one-way analysis of variance (ANOVA) followed by Bonferroni's Multiple Comparison Test and "*" denotes statistical significance (*, $p<0.05$; **, $p<0.01$ and ***, $p<0.001$).

4. RESULTS

In this project, transcriptional and translational regulation of *Kim-1* gene was investigated under chemotoxic stress of three xenobiotics OTA, CP and GM. Since different xenobiotics would have different effects on the viability, proliferation and survival of each cell type; it is necessary to measure these effects and decide on optimum concentrations for treatment in HK-2 cell line. It was previously shown that OTA binds to serum albumin [41], for this reason we have performed our experiments both in 10% FBS and serum free conditions to see if presence or absence of serum affects the results. Since no information was available in literature about the interaction of CP and GM with serum proteins, the following assays for these xenobiotics were also performed in 10% FBS and serum free media.

4.1. Viability Assay

HK-2 cells were seeded at a density of $5x10^3$ cells/100μl per well on 96-well plates with clear bottoms. 24 hours later media were removed and cells were treated with 0.1 μM, 1 μM, 10 μM, and 20 μM OTA; 6.725 μM, 12.5 μM, 25 μM, 50 μM CP and 250 μg/ml, 500 μg/ml, 750 μg/ml, 1000 μg/ml GM in 10% FBS and serum free media. XTT cell viability assays were performed as described in methods to assess the effect of xenobiotics OTA, CP and GM on viability of HK-2 cells in a time and concentration dependent manner. Cell viability was calculated according to the formula described in the methods and the results were normalized to control cells of the same group.

It was expected to see a decrease in viability of cells after toxic treatment which was consistent with our results. For cells treated in serum free medium, cell viability was significantly decreased to 79.1 $\pm$ 1.1 percent of control cells after treatment with 1 μM; 67.2 $\pm$ 1.2 percent of control cells after treatment with 10 μM and 52.7 $\pm$ 2.9 percent of control cells after treatment with 20 μM OTA, while no significant effect was observed up to 0.1 μM OTA treatment for 24 hours (Figure 4.1).

For cells treated in 10% FBS medium, the cytotoxic effect of OTA only becomes significant at 10 μM concentration with a decrease of cell viability to 82.7% $\pm$ 0.9 of control cells. This fact further proved the attenuation of OTA's effect by serum albumin. After 20 μM OTA treatment, viability of HK-2 cells decreased to 67.5 $\pm$ 0.4 of control cells.

Viability assays were also performed after 48 and 72 hours of treatment with cells cultured both in 10% FBS and serum free media. The viable cell percentages compared to control cells followed a similar decreasing pattern with increased dosage of OTA both in 48 and 72 hours. However the decrease of viability became more dramatic with increasing time in serum free media.

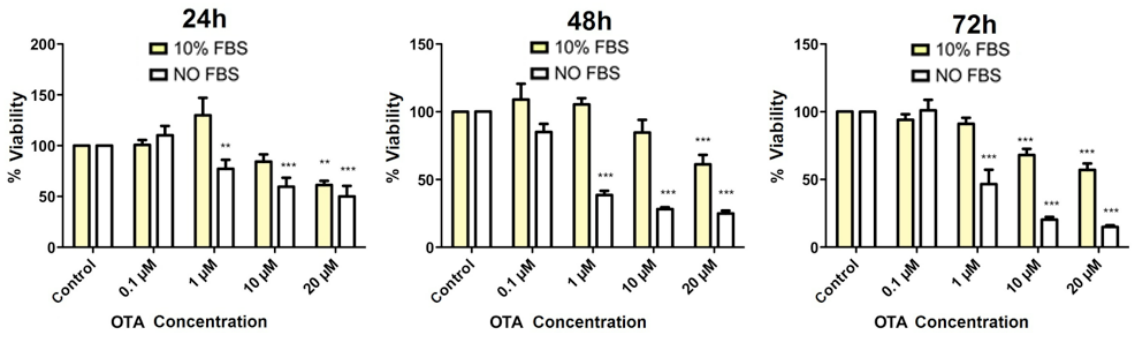

Figure 4.1. Effect of OTA on cell viability in HK-2 cells in 10% FBS and serum free media at different time points. Viability is calculated according to the formula described in the methods (*, $p<0.05$; **, $p<0.01$ and ***, $p<0.001$).

Cell viability gradually decreased below 40 percent of control cells when CP concentration was increased up to 50 μM and the effect of CP treatment on cell viability was significant with 25 μM and 50 μM concentrations (Figure 4.2). For cells treated in 10% FBS medium at 25 μM concentration, viability decreased to 53.1% $\pm$ 2.9 of control cells and for cells treated without FBS in their medium, viability was 54.8% $\pm$ 1.0 of control cells. At 50 μM concentrations viability was 39.8% $\pm$ 1.2 of control cells for 10% FBS and 36,7% $\pm$ 1.0 in serum free media. Viability percentages were similar between cells that were cultured in 10% FBS and in serum free media when

compared to their respective control cells and the difference between them was not statistically significant. Thus, the presence or absence of FBS had no apparent effect on cytotoxicity of CP. When the duration of treatment is increased up to 48 and 72 hours, viability further decreased as expected.

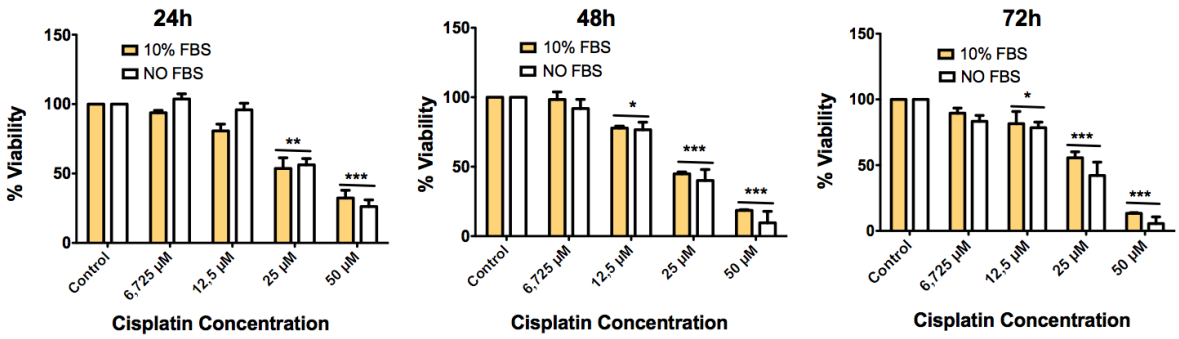

Figure 4.2. Effect of CP on cell viability in HK-2 cells in 10% FBS and serum free media at different time points. Viability is calculated according to the formula described in the methods (*, $p<0.05$; **, $p<0.01$ and ***, $p<0.001$).

In cells treated with GM, viability decreased in a linear manner in 10% FBS and serum free media (Figure 4.3). In 24 hours, when concentration of GM increased up

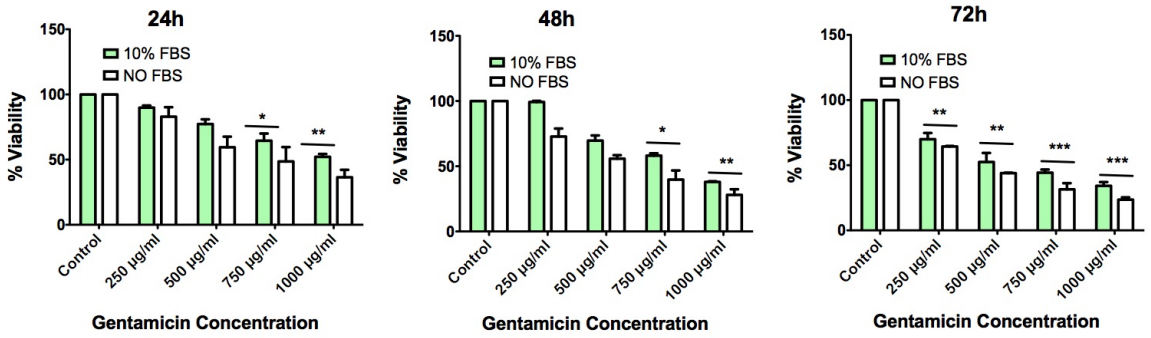

Figure 4.3. Effect of GM on cell viability in HK-2 cells in 10% FBS and serum free media at different time points. Viability is calculated according to the formula described in the methods (*, $p<0.05$; **, $p<0.01$ and ***, $p<0.001$).

to 750 μg/ml in the medium, there was a significant decrease in viability to 72.4% $\pm$ 1.2 of control cells which was also observed at 48 hours with 62.7% $\pm$ 0.3 in 10% FBS medium. In the absence of FBS, viability further decreased to 51.7% $\pm$ 3.4 at 750 μg/ml concentration for 24 hours and to 45.3% $\pm$ 1.4 for 48 hours. When GM concentration is 1000 μg/ml in the medium, viability was measured as 51.3% $\pm$ 0.3 of the control cells for 10% FBS and 40.6% $\pm$ 1.4 of control cells for serum free media after treatment for 24 hours. Viability decreased further to 37.1% $\pm$ 0.1 of control cells in 10% FBS medium and 32.6% $\pm$ 0.5 in serum free medium after 48 hours. If viability was measured 72 hours after treatment, a decrease was observed in all treated samples with or without serum in the media, starting with 250 μg/μl concentration.

4.2. BrdU Proliferation Assay

BrdU proliferation assay measures the rate of proliferation in a given time interval. Since the proteins and growth factors in the serum are required for cells to proliferate, these experiments were conducted only in 10% FBS medium for 24, 48 and 72 hours.

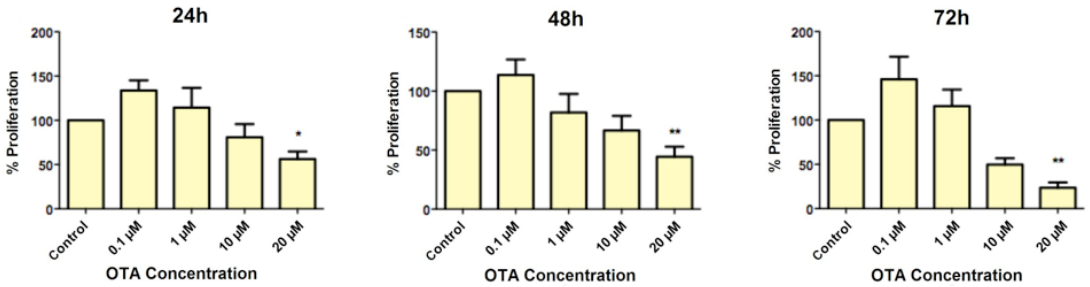

Figure 4.4. Time and concentration dependent effects of OTA on proliferation of HK-2 cells. Results are plotted as standard error of means ($\pm$ SEM) and normalized to control cells (*, $p<0.05$ and **, $p<0.01$).

HK-2 cells were seeded at a density of $5x10^3$ cells/100μl per well on 96-well plates with white bottoms. Then, 24 hours later media were removed and cells are treated with 0.1 μM, 1 μM, 10 μM and 20 μM OTA; 6.725 μM, 12.5 μM, 25 μM, 50 μM CP and 250 μg/ml, 500 μg/ml, 750 μg/ml, 1000 μg/ml GM in 10% FBS

medium. Cells were first treated with the respective xenobiotic for 24, 48 and 72 hours and then incubated with BrdU for 4 hours for labelling. During DNA replication BrdU incorporated into newly synthesized strands in place of thymidine and specific monoclonal antibodies were used to detect cells that were in the S phase of cell cycle. Cells were then fixed and incubated with anti-BrdU peroxide dismutase (POD). After subsequent washing steps the subsrate was added and degraded by POD enzyme which results in chemiluminescence.

For all time intervals there was a significant decrease in proliferation for 20 μl OTA. Although not significant, there was also a slight increase in proliferation for lower doses (0.1 μl and 1 μl) of OTA treatment at all the time points BrdU assay has been performed (Figure 4.4).

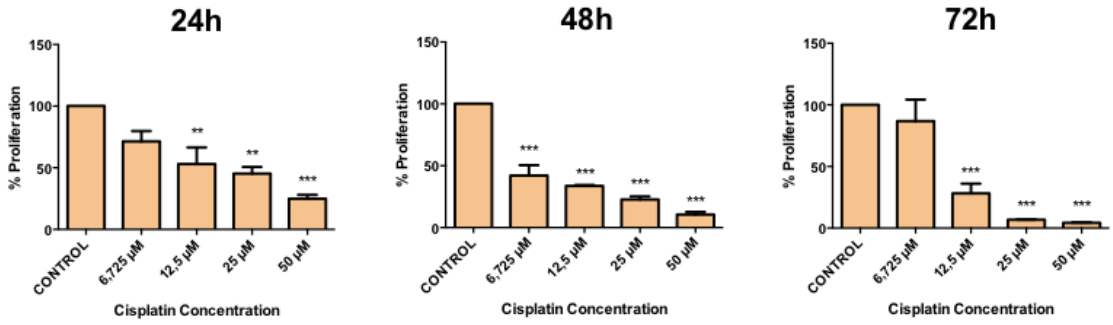

Figure 4.5. Time and concentration dependent effects of CP on proliferation of HK-2 cells. Results are plotted as standard error of means (± SEM) and normalized to control cells (*, $p<0.05$; **, $p<0.01$ and ***, $p<0.001$).

CP treatment caused a decrease in proliferation in time- and dose-dependent manner which was an expected result as CP is used for cancer chemoterapy and targets cells that are proliferating. A significant decrease was detected at 12,5 μM, 25 μM and 50 μM concentrations for 24 hours, 6.725 μM, 12.5 μM, 25 μM, 50 μM concentrations for 48 hours and 12.5 μM, 25 μM, 50 μM concentrations for 72 hours (Figure 4.5).

GM is an antibiotic that targets translation in bacteria and mammals. In cell

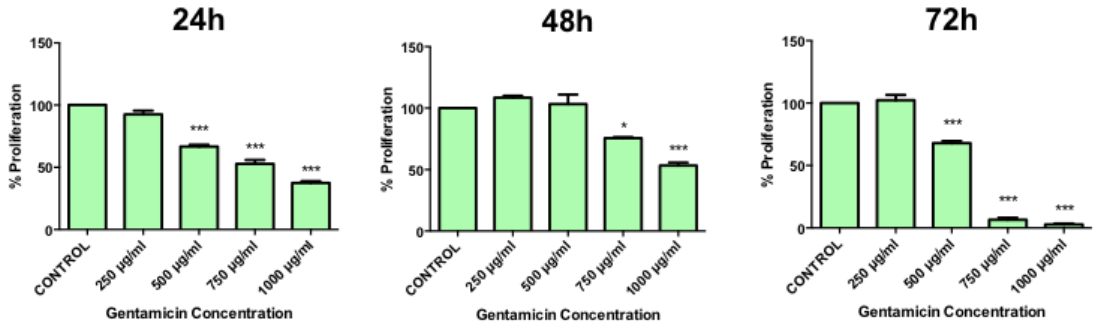

Figure 4.6. Time and concentration dependent effects of GM on proliferation of HK-2 cells. Results are plotted as standard error of means (± SEM) and normalized to control cells (*, $p<0.05$; **, $p<0.01$ and ***, $p<0.001$).

culture, lower dosages of antibiotics are used to prevent contamination and can be tolerated by cells. However, when the cells were exposed to higher dosages of GM for longer periods of time, it is expected to see some decrease in proliferation which was consistent with our results. A significant decrease was observed at 500 μg/ml, 750 μg/ml, 1000 μg/ml concentrations for 24 hours, 750 μg/ml, 1000 μg/ml concentrations for 48 hours and 500 μg/ml, 750 μg/ml, 1000 μg/ml concentrations for 72 hours (Figure 4.6).

4.3. Xenobiotic Induced Necrotic Cell Death

HK-2 cells were seeded at a density of $5x10^3$ cells/100μl per well on 96-well plates with white bottoms. Then, 24 hours later media were removed and cells are treated with 0,1 μM, 1 μM, 10 μM and 20 μM OTA; 6.725 μM, 12.5 μM, 25 μM, 50 μM CP and 250 μg/ml, 500 μg/ml, 750 μg/ml, 1000 μg/ml GM in 10% FBS and serum free media. Cytotox-Glo Assay assay measures the protease activity released by necrotic cells that lost the integrity of their membrane. Since these proteases have relatively short half-lifes, this assay was used only for 24 hr treatments.

Necrosis started at 1μM OTA concentration for cells that were cultured in serum free medium and the ratio of cells that undergo a necrotic death increased up to 10%

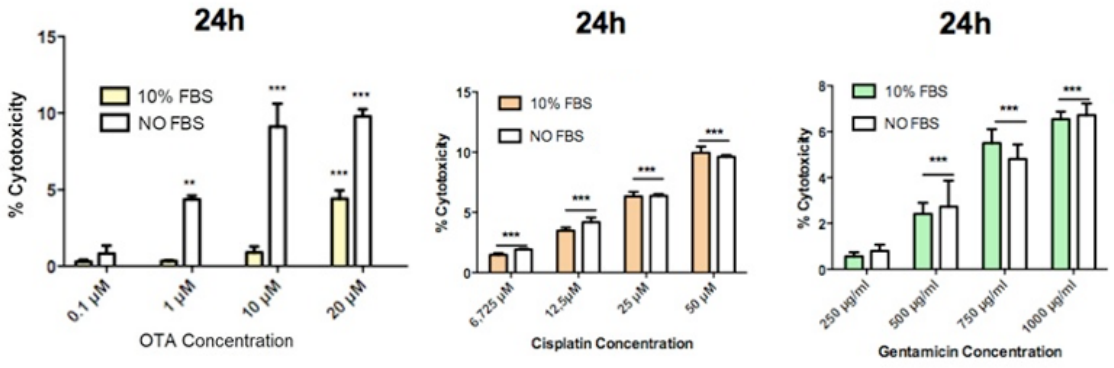

Figure 4.7. Effect of OTA, CP and GM on necrotic cell death in HK-2 cells. Cytotoxicity is calculated by using the formula described in the methods (**, $p<0.01$ and ***, $p<0.001$).

at 20 μM (Figure 4.7). When cells were cultured with 10% FBS, lower OTA concentrations did not cause a significant impact on necrosis. A significant increase in necrosis could only be detected at 20 μM OTA concentration, further supporting the attenuation of OTA's effect due to OTA's interactions with serum albumin. Even at 20 μM concentration, necrotic cell death was 5% in 10% FBS-containing medium, half of what was observed for cells treated in serum free media.

As CP is a strong chemotherapy drug, it induces necrosis even at lower concentrations. A significant increase in necrosis was observed at all concentrations ranging from 6.75 μM to 50 μM both in the presence and absence of serum. Since there is no information about CP's interactions with serum proteins, we performed this assay under both conditions and concluded that presence or absence of serum does not change the outcome of the experiment.

When cells were treated with GM, necrotic cell death again increased in a dose dependent manner starting from 500 μg/ml concentration. At 500 μg/ml necrocity is approximately 3% and it gradually increased up to 7.5% at 1000 μg/ml which was moderate compared to OTA and CP's effect.

4.4. Xenobiotic Induced Apoptotic Cell Death

HK-2 cells were seeded at a density of 5x10^3 cells/100μl per well on 96-well plates with white bottoms. Then, 24 hours later media are removed and cells are treated with 0.1 μM, 1 μM, 10 μM OTA, 6.725 μM, 12.5 μM, 25 μM, 50 μM CP and 250 μg/ml, 500 μg/ml, 750 μg/ml, 1000 μg/ml GM in 10% FBS and serum free media, and apoptotic cell death was measured using Caspase 3/7-Glo Assay.

Although we could see an increase of caspase 3/7 activity starting with cells that were treated with 1 μM OTA, it only became statistically significant at 10 μM concentration (Figure 4.8). For CP, there was a gradual increase of caspase 3/7 activity which became significant at higher dosages such as 25 μM and 50 μM. There was again a gradual increase of apoptotic activity in cells treated with GM and it became significant when the dosage was increased to 1000 μg/ml. From these results we can conclude that all three xenobiotics we used (OTA, CP and GM) trigerred some apoptotic activity in a dose dependent manner.

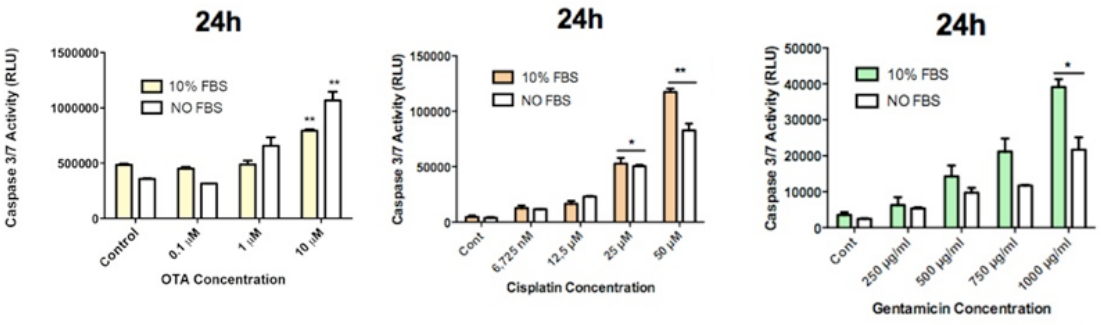

Figure 4.8. Effect of OTA, CP and GM on triggering apoptosis in HK-2 cells. Results are plotted as Standard Error of means (±SEM) and normalized to control cells (*, $p<0.05$ and **, $p<0.01$).

In summary, the following information can be inferred from the above experiments: When cells were cultured in 10% FBS, a significant decrease in viability and proliferation was only detected after treatment with 20 μM OTA for 24 hours. More-

over, 20 μM OTA concentration was needed to cause a significant percentage of cells to undergo apoptosis and necrosis. On the other hand, when the cells were cultured without serum, the effects appeared at lower dosages. For instance, viability significantly decreased and necrotic cell death started at 1 μM concentration, whereas 10 μM OTA treatment was necessary to trigger a significant apoptotic response 24 hours after treatment.

Since CP does not interact with serum proteins, the cells that were cultured in 10% FBS or serum free media generated similar responses to the drug. Twenty-five μM CP was needed to cause a significant decrease at cell viability whereas proliferation diminished significantly upon treatment with 12.5 μM of CP. Furthermore, cells began to undergo necrosis and apoptosis when treated with 6.25 μM and 25 μM CP, respectively. These fluctuations between the concentration rates were generated due to differential sensitivities of the assays. Nevertheless, 25 μM of CP concentration was able to trigger necrosis and apoptosis while abolishing cell viability and proliferation significantly, with or without serum in 24 hours.

Similar to CP, GM also does not interact with serum proteins and results obtained from serum free samples were similar to those obtained from cells that were cultured in the presence of 10% FBS. It was possible to detect necrosis and a decrease in proliferation at 500 μg/ml however viability started to decrease around 750 μg/ml concentration. A decrease in proliferation and necrotic death would lead to a decrease in viability as well at 500 μg/ml concentration but probably due to the sensitivity of the XTT Assay, we were only able to detect a significant decrease in viability at higher dosages. Apoptotic activity started at 1000 μg/ml concentration and approximately 1/3 of caspase activity was detected compared with CP and OTA's higher dosages. This fact suggested that GM may be triggering a necrotic cell death rather than a programmed one.

For our experiments with transcriptional and translational regulation of KIM-1, we needed cytotoxicity inducers that would trigger necrosis and apoptosis as well as halting proliferation to a certain degree without overtoxicity. For these reasons, we

have decided to use 20 μM OTA, 25 μM CP and 1000 μg/ml GM concentrations as stress inducers.

4.5. Transcriptional Regulation of KIM-1

4.5.1. KIM-1 mRNA Expression Under Chemotoxic Stress

In order to analyze how KIM-1 mRNA expression changes after treatment with OTA, CP and GM quantitative real time PCR was performed. First, 1x10^6 HK-2 cells were seeded to a 10 cm petri dish. Then, 24 hours later media were removed and cells were treated with 10 μM OTA, 25 μM CP and 1000 μg/ml GM in 10% FBS medium. RNA was isolated 24 hours after treatment using the TriPure Isolation Reagent(Roche) according to the manufacturer's instructions. RNA sample qualities were tested using absorbance values and run on a formaldehide/agarose gel (Table 4.1., Figure 4.9).

Table 4.1. Concentrations and absorbance values of RNA samples isolated after treatment.

	Concentration (ng/μl)	**260/280**	**260/230**
Control	2218	1,87	2,31
OTA	2155	1,90	2,31
Cisplatin	1930	1,98	2,31
Gentamicin	1350	1,96	2,35

cDNA was synthesized using Transcriptor High Fidelity cDNA Synthesis Kit (Roche) according to the manufacturer's instructions and 1/20th of the final solution was used in the following RT-qPCR reactions. For data normalization Hypoxanthine phosphoribosyltransferase 1 (HPRT1) was used as an endegenous control (housekeeping gene) to correct for sample to sample variations in the efficiency of RT-qPCR reactions and errors in sample quantification. Primers were designed specific to each gene (KIM1 and HPRT1) using the QuantPrime software. KIM-1 mRNA levels were measured in

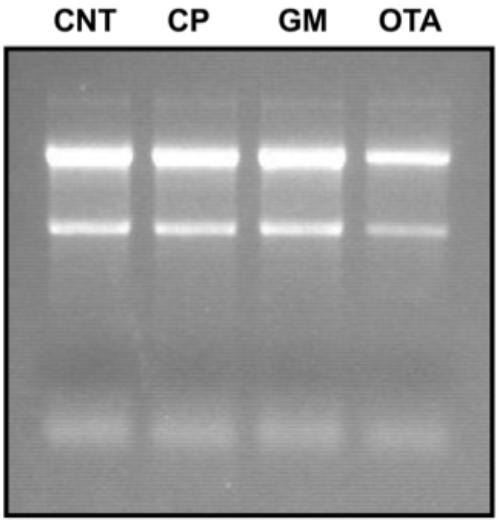

Figure 4.9. An example of formaldehide/agorase gel image of isolated RNAs after treatment with 10 μM OTA, 25 μM cisplatin and 1000 μg/μl gentamicin.

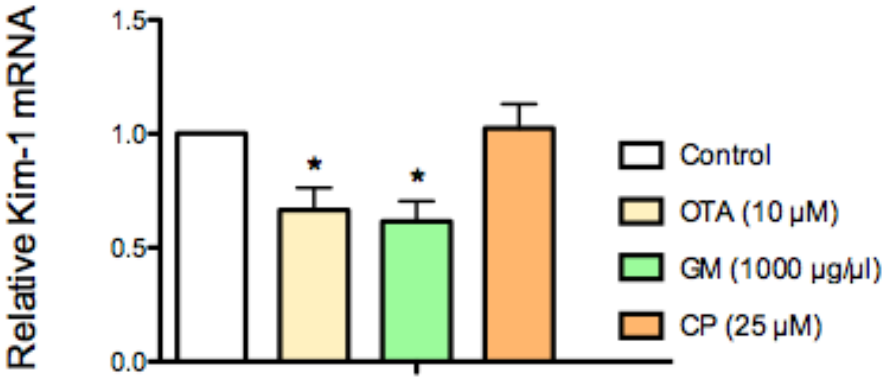

Figure 4.10. Relative quantification of KIM-1 mRNA in HK-2 cells after treatment with 10 μM OTA, 25 μM cisplatin and 1000 μg/μl gentamicin.

triplicates using AccuPower GreenStar qPCR Mastermix. There was a significant decrease in mRNA expresion of KIM-1 after treatment with OTA and GM (33.5% ± 9.7, 38.5% ± 8.9 respectively) whereas samples treated with CP had similar mRNA expression with the untreated control samples (Figure 4.10).

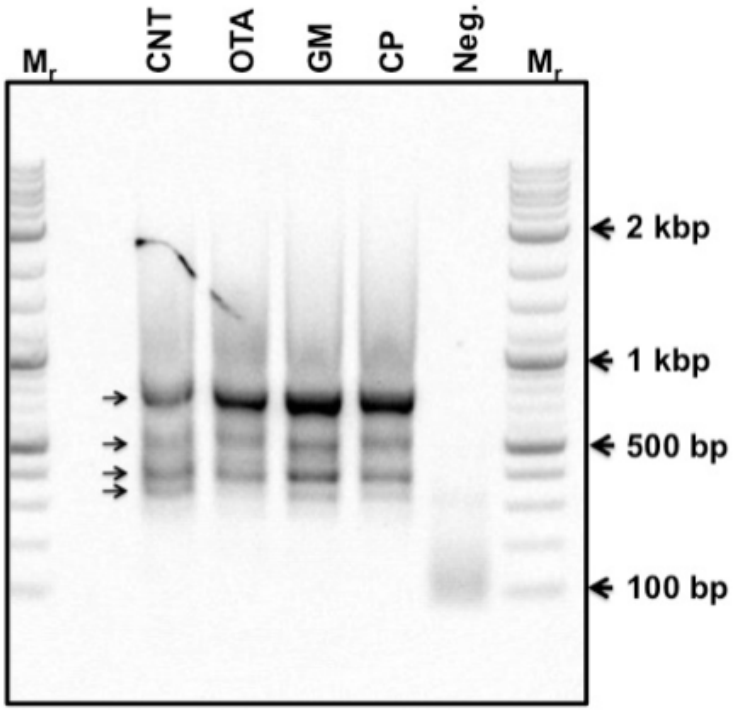

Figure 4.11. Agarose gel image of RLM-RACE Products.

4.5.2. Determination of the Transcriptional Start Site of KIM-1 Gene by RLM-RACE

There are three KIM-1 mRNAs differing in their 5' UTRs until now. All of these three variants code for the same protein with 364 aminoacids and they are thought to arise from alternative splicing. Since these variants were discovered while creating cDNA libraries, they might not start where the transcription starts *in vivo*. In order to characterize the minimal promoter region we first needed to understand where the transcription starts by using the RLM-RACE method.

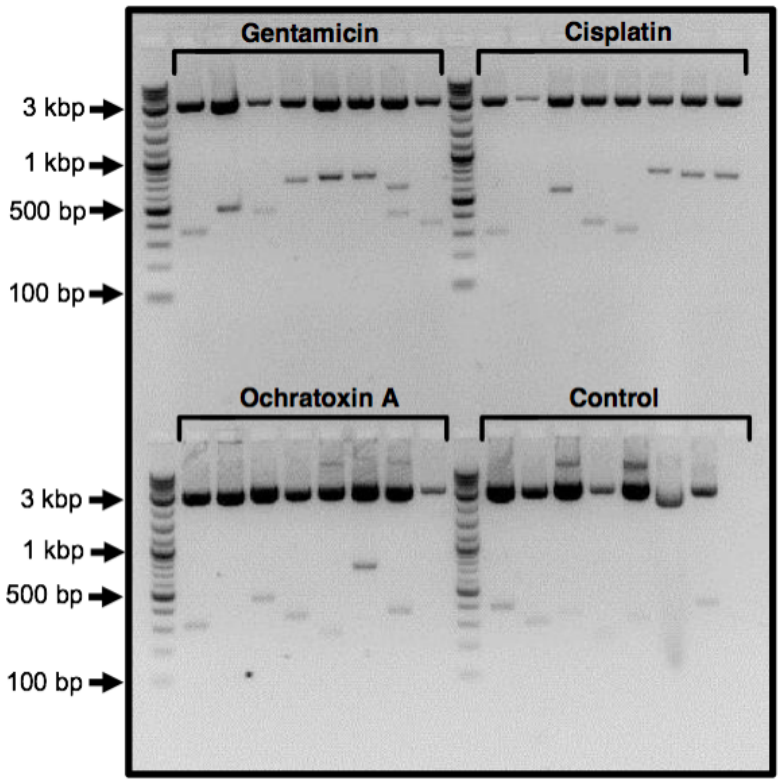

Figure 4.12. Agarose gel image of restriction analysis for the cloning of RLM-RACE products into pGEM-T Easy vector.

To start RLM-RACE experiments we isolated RNA from treated cells. Briefly, 1x10^6 HK-2 cells were seeded to a 10 cm petri dish. Then, 24 hours later media were removed and cells were treated with 10 μM OTA, 25 μM CP and 1000 μg/ml GM in 10% FBS medium. RNA was isolated 24 hours after treatment using the TriPure Isolation Reagent(Roche) according to the manufacturer's instructions. RNA sample qualities were tested using absorbance values and run on a formaldehide/agarose gel. cDNA was synthesized using Transcriptor High Fidelity cDNA Synthesis Kit (Roche) according to the manufacturer's instructions and RLM-RACE was performed as described in the methods. In total four different variants of KIM-1 5'UTR mRNA were detected which are visible on the Figure 4.11. These fragments are 700, 550, 400 and 325 base pairs long. These PCR products were extracted from the gel, purified using Roche High Purification kit and cloned into pGEM-T Easy (Promega) vector.

Eight colonies were selected for each condition including untreated control sample and treatments with three xenobiotics. A gel picture showing the restriction analysis of cloning can be seen at Figure 4.12. Note that products had various lengths in all treated samples. These selected colonies were sequenced and aligned against the previously characterized variants of KIM-1 mRNA and the genomic DNA (Figure 4.13). Among those 5'RLM-RACE products only one variant from the database was detected named OTA 3. Several other variants were also visible which are similar to previously characterized variants but they differ in a few nucleotides. This result led us to believe that the transcription does not start at an exact point instead it starts from a region. This region is depicted at Figure 4.14 and called the transcription start region.

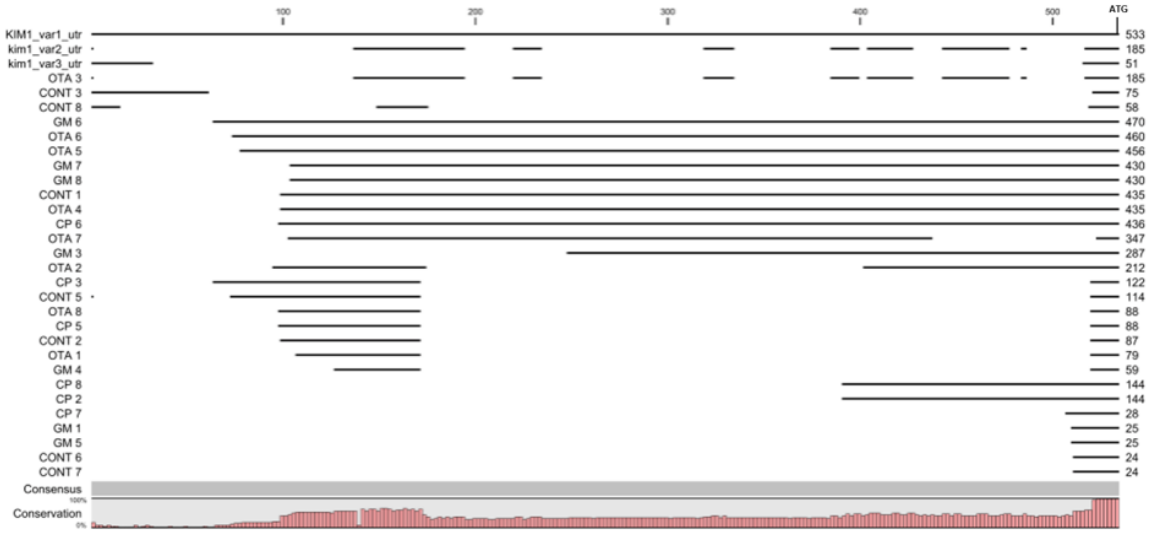

Figure 4.13. Alignment of 5'RACE constructs with the genomic DNA.

4.6. Translational Regulation of KIM-1

In order to understand whether there is a change in KIM-1 protein levels in HK-2 cells after treatment with OTA, CP and GM western blot analysis was performed. First, $1x10^6$ HK-2 cells were seeded to a 10 cm petri dish. Then, 24 hours later media were removed and cells were treated with 10 μM OTA, 25 μM CP and 1000 μg/ml GM in 10% FBS medium. Proteins were isolated 24 hours after treatment and protein concenrations were measured using BCA Protein Assay Kit (Pierce). Expression levels

of KIM-1 protein after treatment with OTA, CP and GM were analyzed by Western blotting. Band intensities were calculated using ImageJ software and normalized to β-Actin.

Figure 4.14. The transcriptional start region of KIM-1 mRNA.

Western blot analysis revealed three bands specific to KIM-1 which have the molecular weight of 40, 60 and 70 kDa (Figure 4.15). These bands were previously characterized as KIM-1 specific bands as 60 and 70 kDa bands were reported to be the glycosylated forms of KIM-1 protein through digestion with CNBr [2]. The seventy kDa band represents the membrane bound form of KIM-1 and changes in the protein level are expected to be observed at this form. Densitometric analysis revealed 18.5, 3.6 and 6.5 fold increase in KIM-1 protein levels compared with control cells in samples treated with OTA, CP and GM, respectively (Figure 4.16).

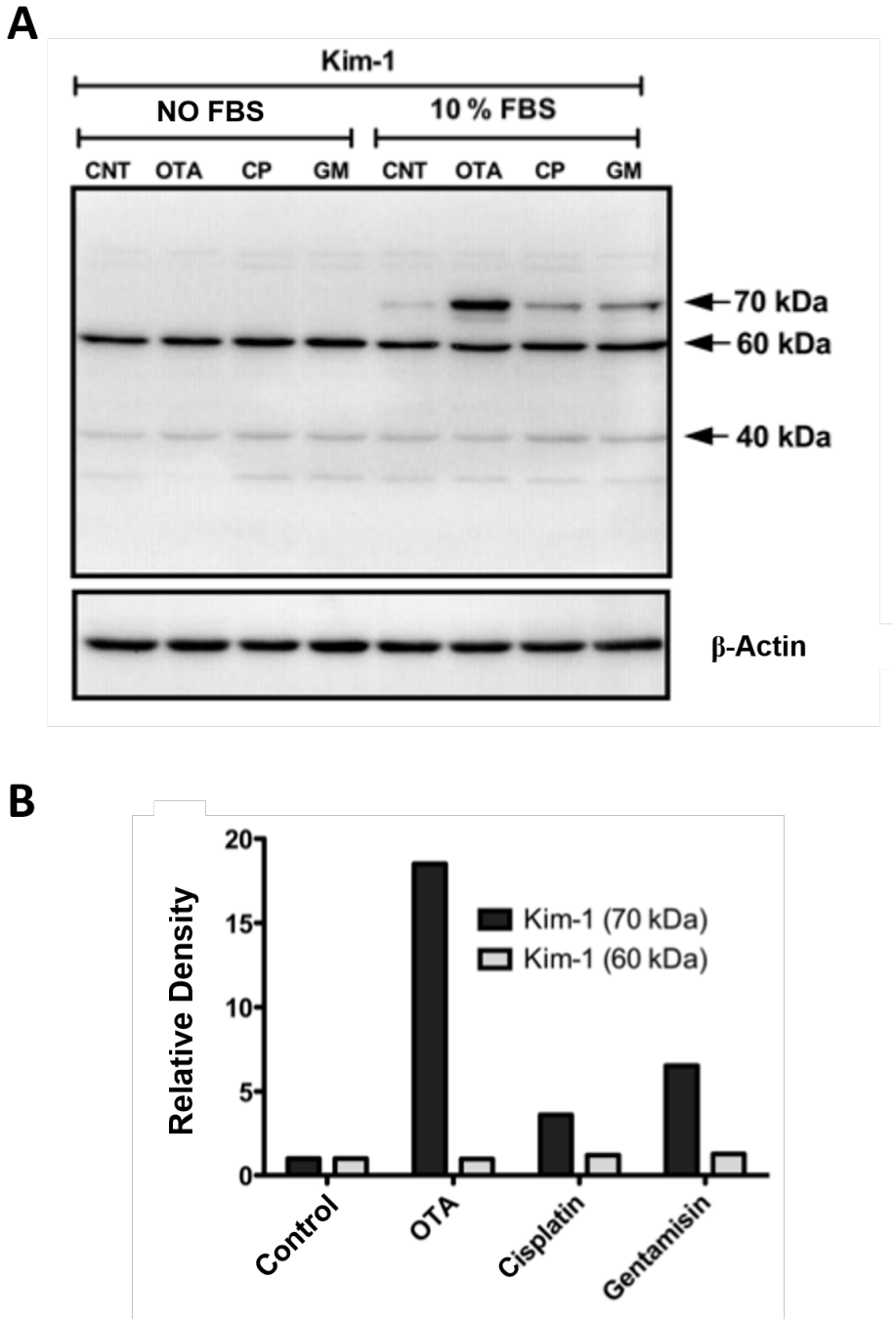

Figure 4.15. Effect of OTA, CP and GM on the expression levels of KIM-1 protein in HK-2 cells. (A) Protein extracts of HK-2 cells that were treated with 10 μM OTA, 25 μM CP and 1000 μg/ml GM. (B) Densitometric analysis of 60 and 70 kDa proteins.

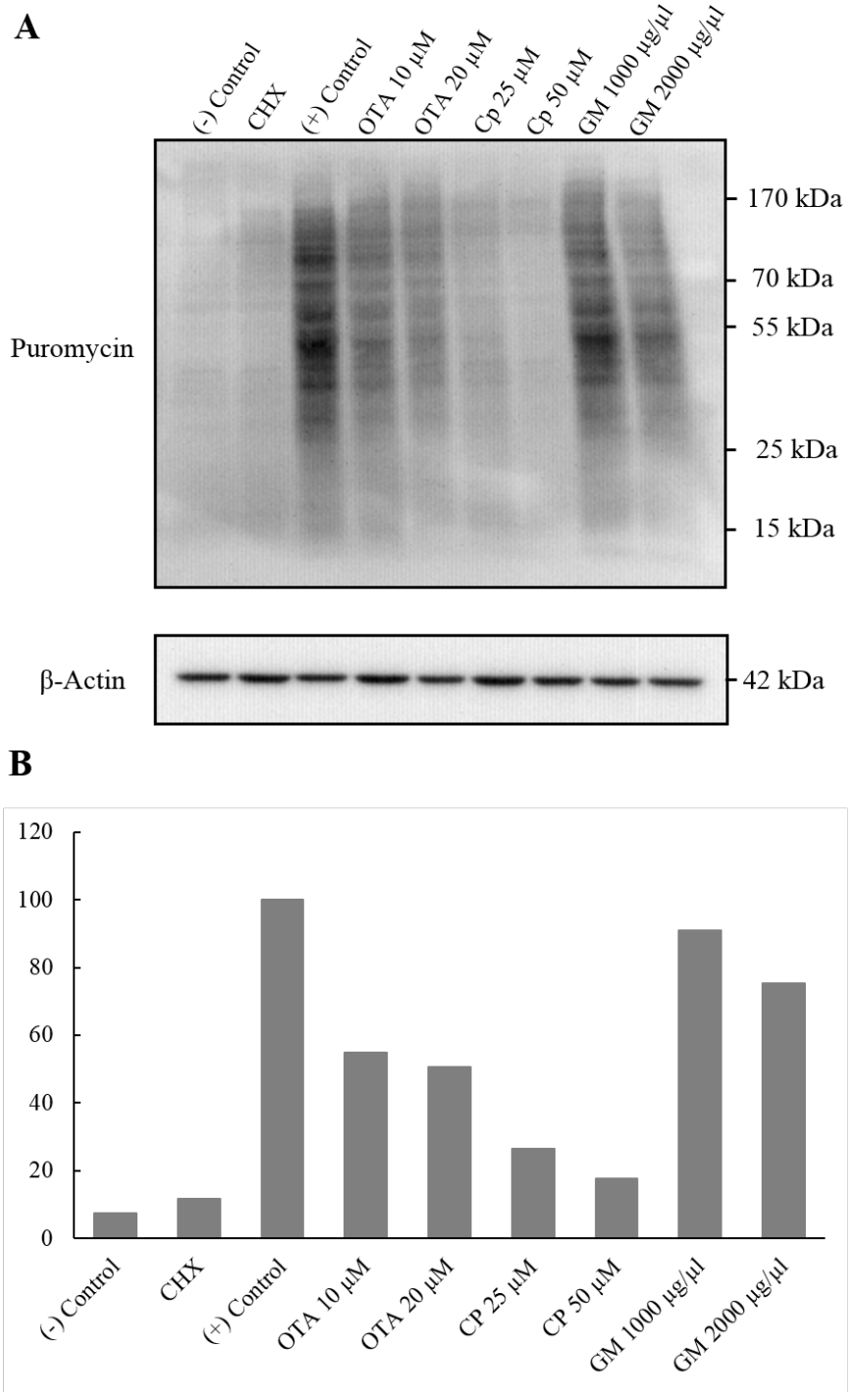

Figure 4.16. Quantification of global protein synthesis after treatment with OTA,CP and GM with anti-puromycin antibody. Band intensities were calculated using ImageJ software and normalized to β-Actin.

There was no visible band at 70 kDa at samples treated in serum free media which was an expected result as KIM-1 expression is correlated with proliferating cells and serum proteins are crucial for triggering proliferation. There was no change in 40 and 60 kDa forms of KIM-1 protein in treated samples compared to control cells.

In order to visualize and quantify global protein synthesis rate after treatment with OTA, CP and GM western blot analysis was performed using anti-puromycin antibody. In addition to treated samples, there was one negative and one positive control along with a sample treated with cyclohexemide (CHX) which is also an inhibitor of protein biosynthesis in eukaryotic organisms. Puromycin, an antibiotic produced by *Streptomyces alboniger*, acts as an analog of aminoacyl tRNAs, thus it prevents the elongation of proteins by getting incorporated into the nascent polypeptide chain (22). It was previously used in minimal amounts to succesfully observe and quantify the rate of mRNA translation *in vitro* (22). The western blot analysis which targets to reveal the impact of xenobiotics to protein synthesis rate consists control lanes that are devoid of puromycin, xenobiotics or both. The negative control sample represents the lysates of cells that are not treated with puromycin and any xenobiotics. This sample is included to the assay as an indicator of anti-puromycin antibody's cross reactivity. Negative control lane did not contain any distinct bands, confirming that the anti-puromycin antibody did not interact with other elements in lysates other than the puromycin itself (Figure 4.17A). On the other hand, the positive control lane revealed a myriad of bands with numerous sizes which represents the global protein of the cell that is being synthesized at the moment of puromycin treatment which halts the protein translation. In order to confirm that the observed smear of proteins are formed due to puromycin's impact on protein translation. Another control was added to the assay for which the cells were pretreated with CHX. CHX is a translation inhibitor and it blocks the incorporation of puromycin into the nascent polypeptide chain. Thus, CHX that is introduced to cells before puromycin treatment should diminish the interaction of puromycin with proteins and drastically decrease the intensity of the bands. As expected, the intensity of the bands in the CHX lane was only 11.7% of the positive control proving that puromycin exclusively labels nascent polypeptides (Figure 4.17B). After treatment of cells with xenobiotics, global protein translation rate gradually de-

creased in a dose dependent manner. For instance, due to treatment of cells with 10 μM OTA, the intensities of the bands decreased to 54.9% of the positive control lane. When the concentration of OTA is increased to 20 μM, the intensity of the bands was further decreased to 50.7% of the control indicating that the impact of the xenobiotic on total protein translation is dose dependent. This dose dependent impact became more evident after CP treatment. 25 μM of CP diminished protein translation to 26.4% of the control and upon the increase in its concentration to 50 μM the percentage of band intensities became 17.6% of the control lane. Finally, 1000 and 2000 μg/ml of GM lead to a decrease in global protein sythesis at 91% and 75.3% of the control lane, respectively.

In summary, there was a significant decrease in mRNA expresion of KIM-1 after treatment with OTA and GM and in samples treated with CP mRNA expression level remained the same with untreated control samples. Furthermore, when total protein levels were quantified in cells after treatment with all three xenobiotics a significant decrease was observed in a dose dependant manner. Curiously, KIM-1 protein levels were observed to increase after treatment with OTA, CP and GM where global protein synthesis rate decreased. These findings led us to suspect that there might be a translational regulatory mechanism controlling the KIM-1 protein expression. One of the most prominent ways of translational regulation mechanism is the use of an Internal Ribosome Entry Site (IRES). To test for the presence of an IRES we performed further experiments.

4.7. ASSESSING IRES ACTIVITY

The most common method to assess IRES activity is to use bicistronic expression vectors [35]. Unless there is an IRES sequence between two reporter genes, the ribosomes would translate the first reporter protein and fall off from the bicistronic mRNA when they reach a stop codon. However, if the insert that is cloned between two reporter genes contains an IRES sequence, the ribosomes may use this structure to dock again onto the mRNA and translate the second reporter protein (Figure 4.17). IRES activity is measured by calculating the ratio of reporter protein 2 to reporter

protein 1.

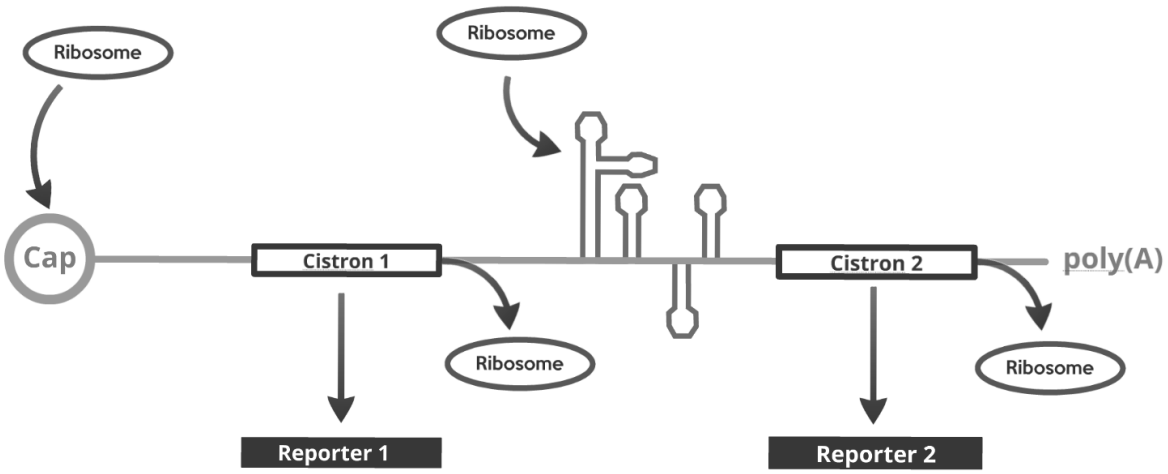

Figure 4.17. mRNA product of bicistronic expression vectors and possible ways of its translation.

As a bicistonic expression vector we used pRF which contains Renilla and Firefly luciferases as reporter genes, a multiple cloning site in between and SV40 promoter and enhancer sequences to drive the transcript. In order to obtain 5'UTR of KIM-1 mRNA, a primer pair targetting variant 1 in NCBI database was designed and cDNA obtained from HK-2 cells was used as a template. Two different sequences containing the 5' UTR of KIM-1 gene were obtained, named as KIML and KIMS and cloned into the multiple cloning site of pRF using NcoI and EcoRI sites. Consensus sequences of KIML and KIMS can be seen at Figure 4.18. As a positive control, previously characterized encephalomyocarditis virus (EMCV) IRES sequence was used (Figure 4.19).

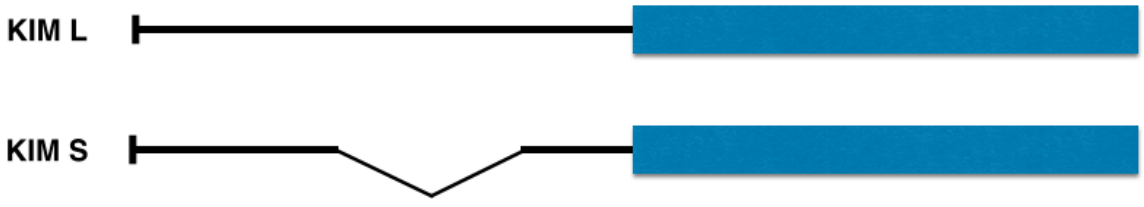

Figure 4.18. Consensus sequences of KIML and KIMS.

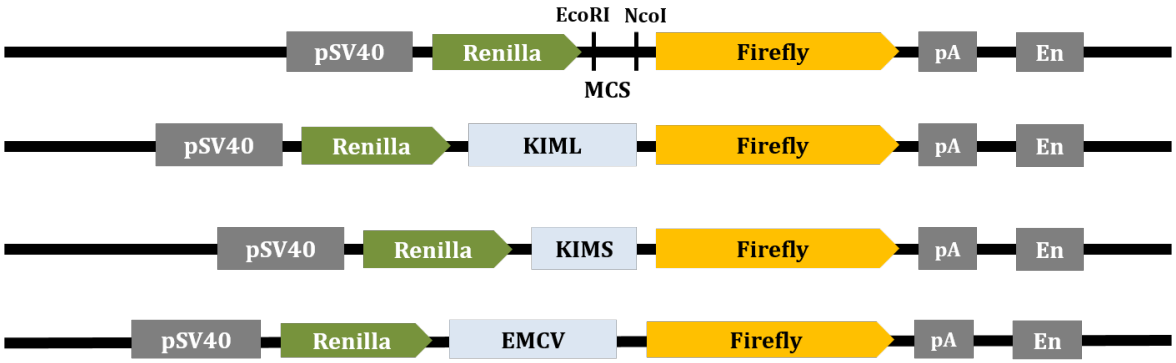

Figure 4.19. Bicistronic expression vectors used in *in vitro* transfections into HK-2 cell line.

pRKIMLF and pRKIMSF along with negative control pRF and positive control (pREMCVF) were transfected into HK-2 cells as described in the methods and luciferase activity was measured using Dual Luciferase Assay from Promega. Firefly/renilla ratios were calculated, normalized to empty vector and used for assessment of IRES activity. It was generally observed that transfection of the empty control vector pRF into cultured cells will result in high levels of renilla luciferase activity, but almost none or severly reduced firefly luciferase activity due to lack of translation of the second cistron. If 5' UTR of KIM-1 has IRES activity in HK-2 cells, high levels of firefly luciferase activity in addition to renilla luciferase activity is to be expected. As foreseen, EMCV transfection resulted in 17 ($\pm$0.9) fold increase in firefly/renilla ratios compared to the empty vector pRF. KIMS was able to mimic the fold increase of EMCV IRES with 17.4 ($\pm$3.6) whereas the ratio of firefly to renilla was even higher for KIML: 68.1 ($\pm$4.2) (Figure 4.20).

This approach has been claimed to be compromised by the possible occurance of cryptic promoter activity, splicing and possible rearrangement of reporter genes [35]. In order to test these possibilities, we removed the minimal SV40 promoter region of the pRF vector (Figure 4.21). Unexpectedly, after removal of the minimal SV40 promoter region some firefly activity remained although renilla activity had completely vanished. The remaining firefly activity detected in promoterless constructs was much less compared to intact vectors, 75% decrease for KIMS and 72% for KIML (Figure

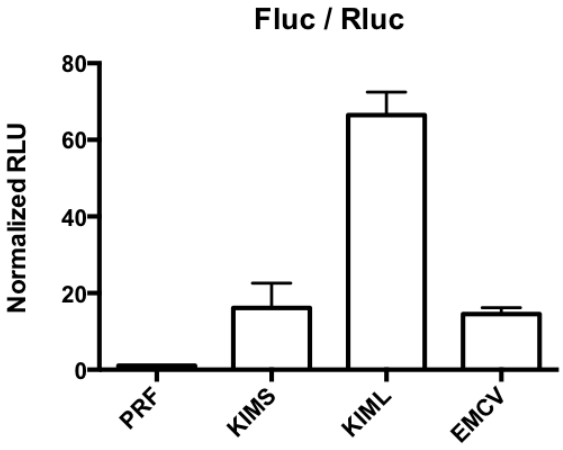

Figure 4.20. Normalized Firefly/Renilla luciferase ratios.

4.22).

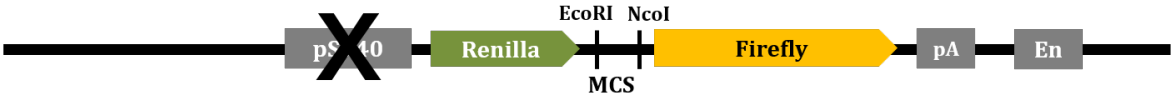

Figure 4.21. Promoterless pRF vector.

A literature search led us to suspect that the remaining enhancer region might cause cryptic promoter activity from the inserts [42] or firefly luciferase gene [43]. To test this hypothesis, we created enhancerless and enhancerless and promoterless vectors (Figure 4.23, Figure 4.24). Removal of the enhancer is expected to reduce the amount of bicistronic mRNA produced but the ratio of firefly to renilla luciferase should not change assuming they are both translated from a single bicistronic mRNA [42]. This was in fact what we observed, EMCV transfection resulted in 7,57 (±0.23) fold increase in firefly/renilla ratios compared to the empty enhancerless vector ΔEpRF. KIMS had 4,66 (±0.53) times more firefly activity than the enhancerless pRF whereas the normalized ratio of firefly to renilla of KIML is 9 (±0.56; Figure 4.25).

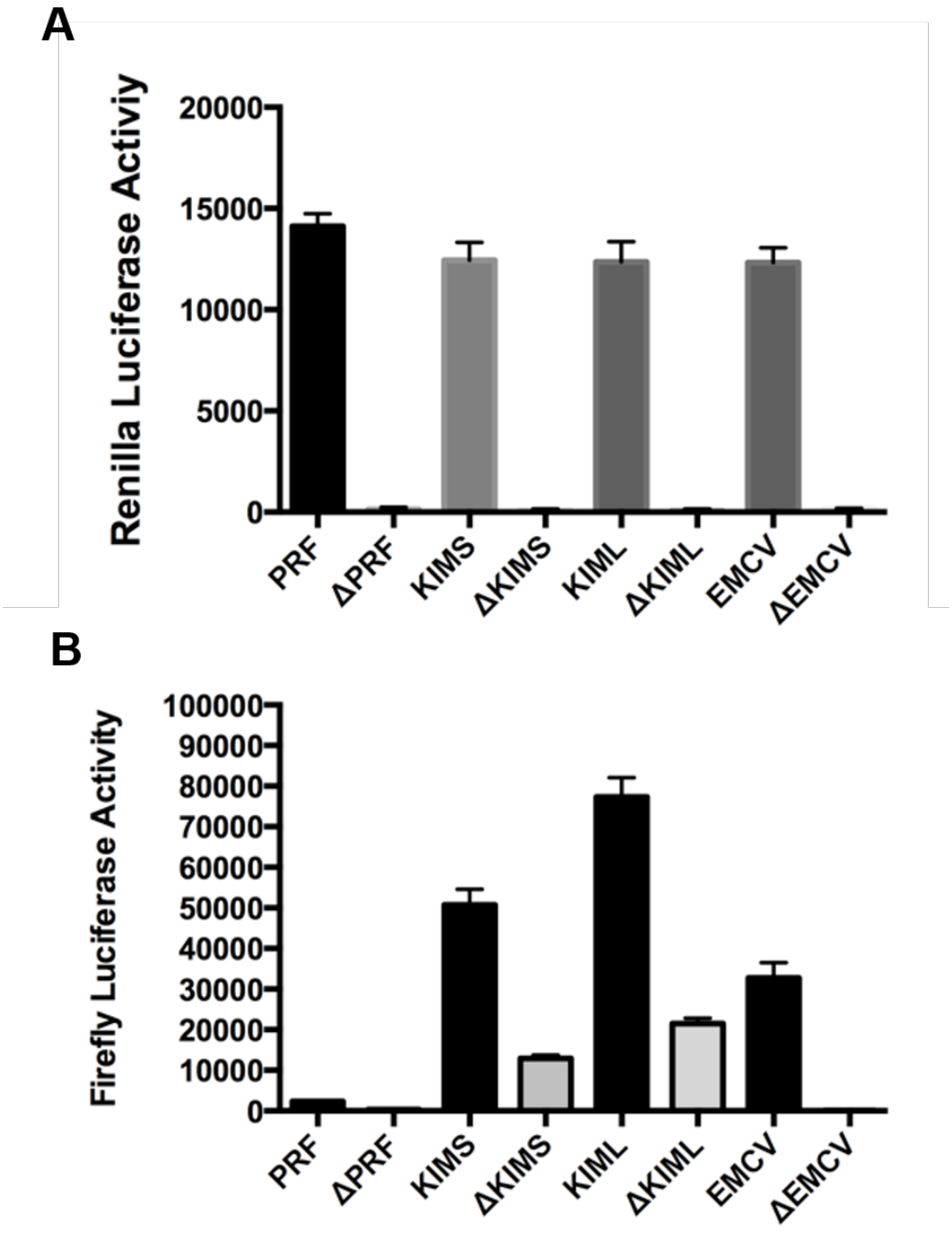

Figure 4.22. Comparison of (a) renilla and (b) firefly luciferase activities in the presence and absence of minimal SV40 promoter.

Figure 4.23. Enhancerless pRF vector.

Figure 4.24. Enhancerless and promoterless pRF vector.

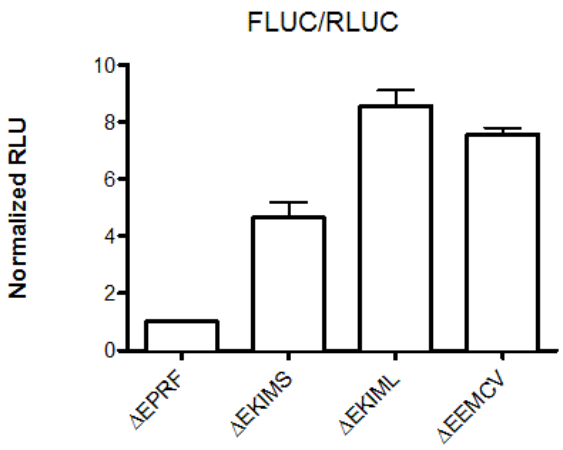

Figure 4.25. Normalized Firefly/Renilla ratios for enhancerless constructs.

Together these results were very similar to what was observed in initial experiments with the intact vectors; however, the fold increases obtained with enhancerless constructs were less than the intact vectors. The removal of the enhancer decreased both the luminescence measured from firefly and renilla and the ratio of firefly to renilla luciferases; strengthening the view that there might be a cryptic promoter activity coming from the constructs but the ratio can not be explained only by cryptic promoter activity (Figure 4.26).

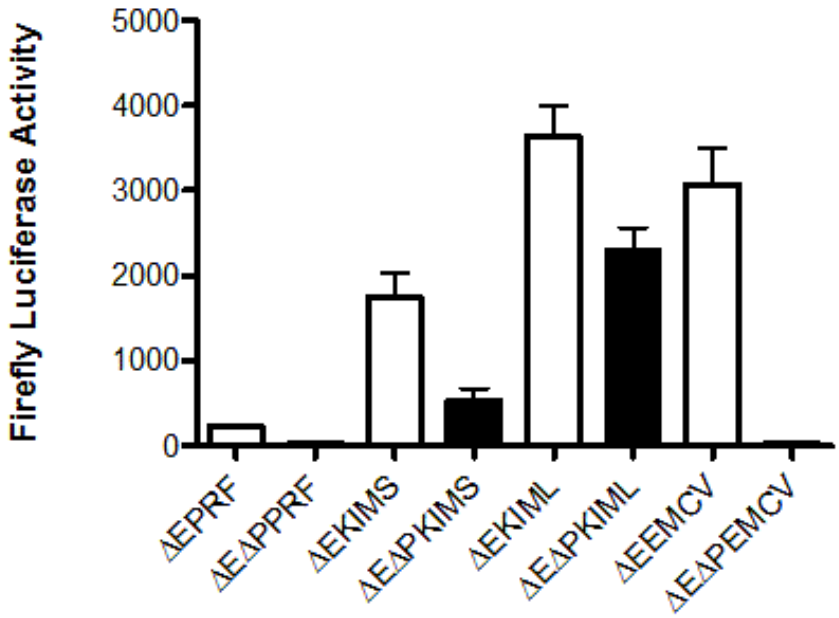

Figure 4.26. Comparison of firefly luciferase activities of enhancerless constructs in the presence and absence of minimal SV40 promoter.

Removal of both the promoter and the enhancer regions eliminated the renilla luciferase as before and decreases firefly luciferases significantly (Figure 4.27). As expected the firefly luciferase dimished for EMCV control and ΔEΔPpRF completely and decreased up to 75% for KIMS but only 38% for KIML. This is reasonable since the longest 5' UTR detected by our RLM-RACE experiments started at 470 bp upstream of the start codon and KIML spans a region upto -537 suggesting it might contain regulatory elements for transcription.

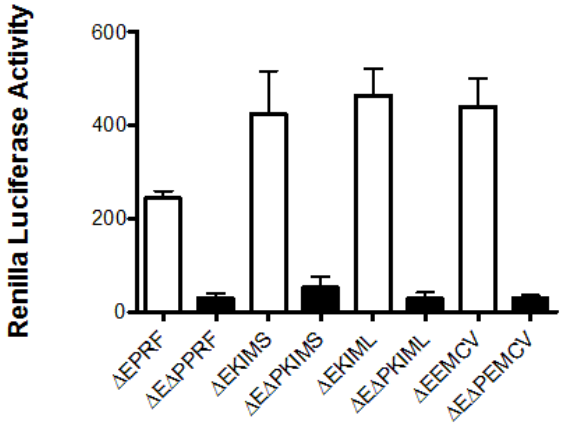

Figure 4.27. Comparison of renilla luciferase activities of enhancerless constructs in the presence and absence of minimal SV40 promoter.

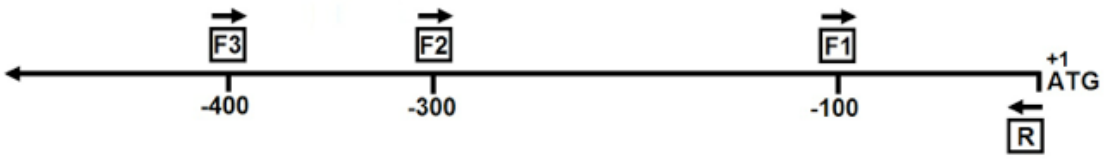

Figure 4.28. Locations of the primers used to generate constructs named pR100F, pR300F and pR400F.

To localize the possible IRES and promoter activity we created constructs comprising 100, 300 and 400 base pairs upstream of the start codon (Figure 4.28). Firefly/Renilla ratios were again calculated, normalized to the empty vector and compared with EMCV. The construct that contained the 100 bp segment resulted in 0.45 Fluc/Rluc ratio suggesting that a possible IRES activity is completely diminished. On the other hand, constructs containing 300 bp and 400 bp segments generated 42.42 ($\pm$4.9) and 62.19 ($\pm$1.3) fold increased FLUC/RLUC ratios compared to the empty vector respectively. This result indicated that both these segments may contain IRES activity. In this system our positive control EMCV transfection resulted in 35.39 ($\pm$2.1) fold increase over pRF whereas KIMS and KIML produced 43.56 ($\pm$7.2) and

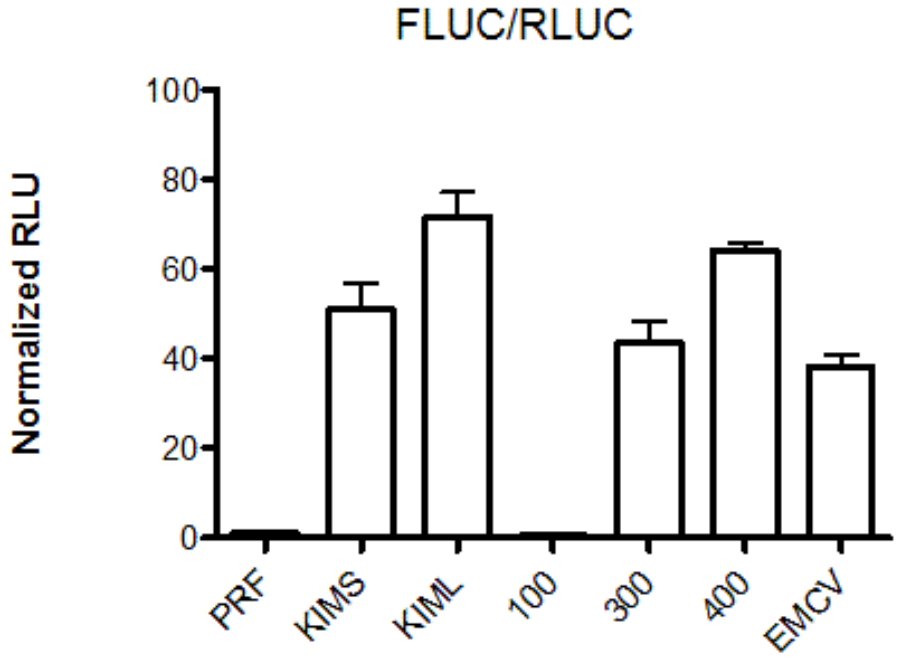

Figure 4.29. Normalized Firefly/Renilla luciferase ratios.

66.57 (±6.9) ratios, respectively. Thus, the possible IRES sequence that gave rise to high FLUC/RLUC ratios in both KIML and KIMS segments were further localized in 300 bp and 400 bp constructs. To test whether these constructs would give rise to any cryptic promoter activity we once again removed the promoter sequence of pRF and obtained promoterless constructs. Once again, all renilla activity diminished in all of the promoterless constructs as expected.

In the promoterless constructs, firefly luciferase activity was calculated to be 443 units for 100 bp segment, 332 units for 300 bp segment and 1897 units for 400 bp segment. The highest value was produced in the construct containing the 400 bp segment and it was in parallel with the firefly luciferase activity of KIML and KIMS: 1652 and 1045 units, respectively. On the other hand, 332 units of firefly luciferase activity detected in 300 bp segment was comparable with pRF and EMCV: 232 and 237 units respectively. The data indicated that the cryptic promoter activity found in KIML and KIMS that leads to high firefly luciferase activity exist on 400 bp segment. However this cryptic promoter activity seems to be eliminated in the 300 bp segment.

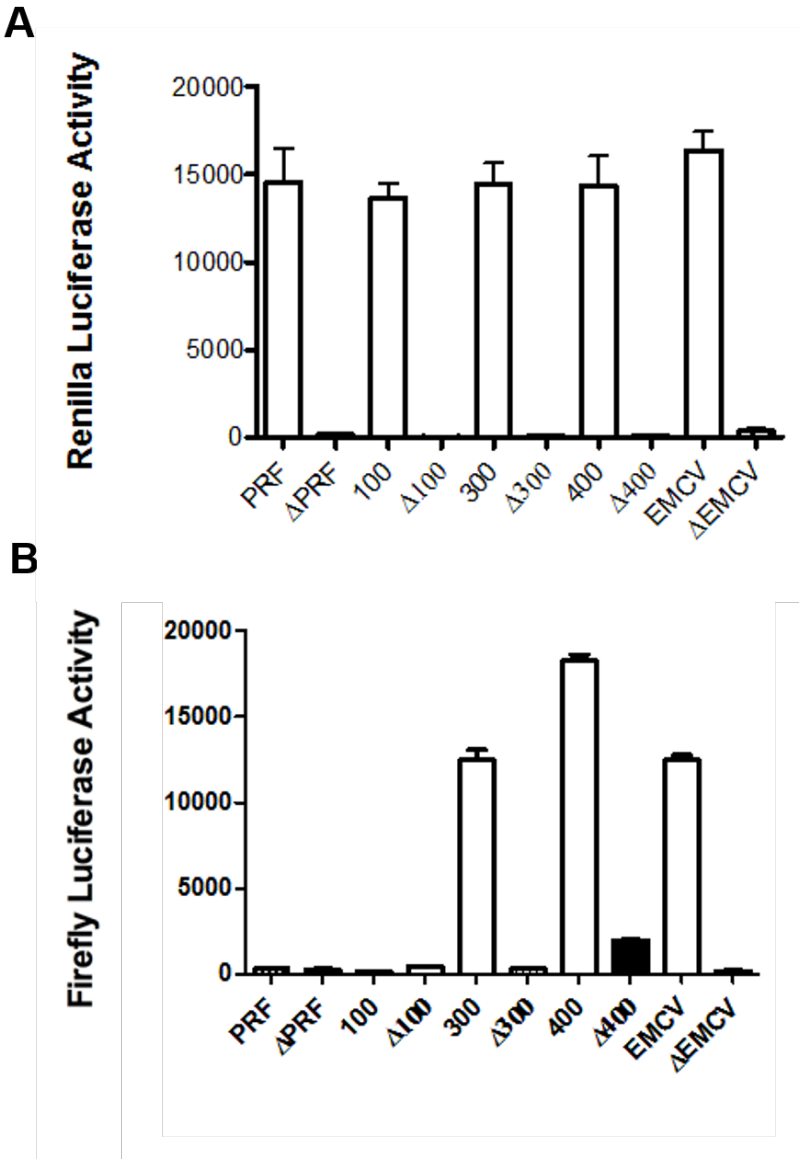

Figure 4.30. Comparison of renilla and firefly luciferase activities in the presence and absence of minimal SV40 promoter.

Thus, the 300 bp segment with reasonable firefly/renilla ratio that is similar to the EMCV IRES and very low levels of firefly luciferase activity in promoterless constructs seems to represent the region where the possible IRES sequence is localized as it is devoid of any cryptic promoter activity.

5. DISCUSSION

In this thesis KIM-1's transcriptional and translational regulation under chemotoxic stress is studied. In order to elucidate the transcriptional and translational mechanisms that regulate KIM-1 gene expression under chemotoxic stress, three different xenobiotics, OTA, CP and GM were used throughout the study.

Using these chemicals and HK-2 cell line a chemotoxic stress induction model was sought to be established. Critically, the duration of the treatment and the concentration of the chemicals were optimized separately for each of these xenobiotics. Determining the right amount of xenobiotics in treatment steps was crucial because the concentrations should be high enough to trigger a stress response in cells while not killing the entire population of cells due to over-toxicity. The second consideration in the chemotoxic stress induction step was the duration of the treatments. In parallel to the use of low concentrations, treatment of cells for a short periods of time may not initiate stress responses from the cells. Thus, the gene regulatory mechanisms that are active during stress conditions will not be triggered. Similarly, the over-exposure of chemicals in treatment step may cause the death of the entire cell population instead of initiating a stress response. Hence, both the duration of treatments and the amount of chemicals used in the treatment step should be optimized and standardized before investigating the KIM-1's regulation via translational or transcriptional mechanisms. In this study XTT cell viability, BrdU proliferation, Cyto-tox Glo and Caspase 3/7 assays were performed for the optimization of chemotoxic induction model.

The XTT cell viability assay measures proliferation but it could also be used to measure viability under chemotoxic stress conditions. To determine the optimum concentrations, XTT cell viability assays were performed for each chemical in serum free and 10% FBS media conditions for 24h, 48h and 72h. BrdU proliferation assay measures the rate of proliferation and this assay was performed to determine the effects of xenobiotics on proliferation of HK-2 cells at 24h, 48h and 72h time points. Since serum was needed for cells to proliferate, these assays were only performed in 10% FBS

medium. Cytotox-Glo assay was performed to determine the percentage of cell death due to necrosis by measuring the protease activity released by the cells that have lost the integrity of their membranes. Since these proteases get degraded after a day, this assay is only performed at 24h time point. Caspase 3/7 activity could also be measured only up to 24 hours and detects activated caspases as a marker of apoptosis. By using both cytotox-glo and caspase 3/7 assays, not only the percentage of cell death was revealed but the method of cell death was also investigated.

As a result of these four assays, The optimal concentrations of these xenobiotics for chemotoxic stress induction were decided to be 10 μM OTA, 25 μM CP and 1000 μg/ml GM. These values were determined considering the percentage of cell death and the whether or not there was a significant effect observable compared to control cells.

After establishing the *in vitro* chemotoxic stress induction model we wanted to reveal the impact of three xenobiotics on total protein synthesis. In order to do that western blot analysis was performed using anti-puromycin antibody. Since puromycin is a substitute of aminoacyl tRNAs it is incorporated into nascent polypeptide chains in protein synthesis process. This incorporation results in termination of the synthesis. Thus, all sizes of proteins which are being synthesized at the moment of puromycin treatment could be detected by using the anti-puromycin antibody. The visualization and quantification of the global protein synthesis rate of different cell populations including the control and the treated samples were performed to reveal the impact of xenobiotics on protein synthesis. The western blot analysis indicated that chemical treatment is resulted in significant decrease in the amount of synthesized proteins under stressful conditions. Band intensities were measured using Image J software and the decrease in global protein synthesis rate was quantified in a dose and chemical dependent manner.

Next, we wondered how KIM-1 protein behaves under the same chemotoxic conditions. Western blot analyses were employed to determine the levels of KIM-1 protein under chemotoxic stress for 24 hours. Three distinct bands were observed at 70, 60 and 40 kDa in size; 60 and 70 kDa bands were reported to be the glycosylated forms

of KIM-1 protein through digestion with CNBr [2]. The seventy kDa band represents the membrane bound form of KIM-1 and changes in the protein level were expected to be observed at this form [1]. Densitometric analysis revealed 18.5, 3.6 and 6.5 fold increase in KIM-1 protein levels in samples treated with OTA, CP and GM, respectively under 10% FBS conditions. The 70 kDa band became invisible at no FBS condition which was an expected result as KIM-1 expression is correlated with proliferating cells and serum proteins are crucial for triggering proliferation. We observed similar results with many studies performed *in vivo* [1, 2, 7] and a similar study performed with HK2 cell line after exposure with oxalate (a metabolic end product excreted by the kidney) where KIM-1 protein amounts increased *in vitro* [13].

As we observed an increase in KIM-1 protein amounts where global protein synthesis rate decreased, we wondered if these finding would correlate with an increase in KIM-1 mRNA levels. KIM-1 mRNA was measured by qRT-PCR, curiously we observed a significant decrease after treatment with OTA and GM where no change was detected after CP treatment. Since the decrease in KIM-1 mRNA levels or the decrease in total protein synthesis were not reflected in KIM-1 protein levels, we suspected that a post-transcriptional regulatory mechanism might be responsible for the increase of KIM-1 protein expression under chemotoxic stress conditions.

One of the main methods of post-transcriptional regulation under stress conditions is the use of an IRES [35]. To test for the possibility of an IRES we first needed to define the transcriptional start site of *Kim-1* gene as the IRESs usually reside in the 5'UTR of an mRNA transcript. In order to define the 5'UTR of the KIM-1 mRNA we performed 5'RLM-RACE experiments. As a result we defined four different 5'UTR variants and described a transcriptional start region instead of a transcriptional start site. Only one of the variants we found was defined in the NCBI database which was called variant number 2. Although we could not detect any variant specific to treatment, the longest variant we could detect was observed to increase in amount with treatment as seen in the Figure 4.11.

In order to test for a possible IRES we created six constructs named pRKIMLF,

pRKIMSF, pR100F, pR300F, pR400F and pREMCVF and transfected these constructs into HK-2 cells. pRKIMLF and pRKIMSF had been amplified from HK-2 cDNA by using primers designed according to the longest 5' UTR variant in the NCBI database. As a positive control, previously characterized and commercially available EMCV IRES sequence was used and the empty vector pRF was used as the negative control. Firefly Luciferase/Renilla Luciferase ratio is used to determine a possible IRES activity [42] and the ratios obtained with both pRKIMLF and pRKIMSF constructs were very similar to pREMCVF. In order to confirm that the firefly activity did not arise from a cryptic promoter residing in our construct, the promoter sequence of pRF is removed. Although the FLUC/RLUC ratios obtained with both pRKIMLF and pRKIMSF were very similar to pREMCVF when the promoter sequences were removed the firefly activity did not diminish as expected. Following this we removed the enhancer and both the enhancer and promoter with a similar strategy described in Bert et al., 2006 [42]. The removal of the enhancer sequence was expected to reduce the amount of bicistronic mRNA produced but the FLUC/RLUC ratio should not change assuming that they are both translated from a single bicistronic mRNA. Our results were as expected, removal of the enhancer sequence reduced the luciferase signal but the FLUC/RLUC ratio was still greater than one and it was in parallel with the ratio calculated in cells that were transfected with pREMCVF. Removal of both the enhancer and the promoter plus enhancer diminished the signals as expected. Consequently, these results were promising enough to further investigate 5' UTR of KIM-1.

For pRKIMLF and pRKIMSF we used primers that are able to amplify the longest transcript described in the NCBI database. In this case, we used primers that can amplify the longest transcript detected in our RLM-RACE experiments and other primers that target shorter fragments. These constructs were named according to their sizes: pR400F, pR300F and pR100F. We also generated promoterless constructs with these amplified regions and transfected each plasmid construct into HK-2 cells. Transfection of the constructs resulted in high FLUC/RLUC ratios for both pR400F and pR300F. However, pR100F construct did not produce much firefly luciferase in transfected cells. Since FLUC/RLUC ratios for both pR400F and pR300F were similar to pREMCVF, we checked the results for promoterless constructs and observed that

the firefly luciferase activity diminished for pR300F construct whereas there was still some remnant firefly activity for pR400F. Consequently, our results suggested that pR300F might contain a functional IRES sequence but further experiments should be performed.

An experimental pitfall about utilization of bi-cistronic transgenic constructs to assess the IRES activity by calculating ratio of reporter protein two to reporter protein one could be the presence of possible monocistronic firefly luciferase transcripts that could elevate the FLUC/RLUC ratios [42]. In order to test for the presence of these monocistronic firefly luciferase transcripts in the transfected cells RNA interference was utilized by Van Eden and his colleagues [44]. In this approach the bicistronic transcript is targeted by RNA interference and theoretically the renilla luciferase activity would be decreased in parallel to the firefly luciferase as these cistrons are on the same mRNA. However, if the firefly activity originates from monocistronic transcripts such as arising from the cryptic promoters residing in the inserts or in the luciferase gene [43] renilla luciferase activity would remain undisturbed. In 2006, Bert *et al.* employed this strategy to the pRF vector system using various different genes and confirmed its use as a test for the presence or absence of monocistronic firefly luciferase transcripts [42]. Consequently, in order to eliminate the possible contribution of monocistronic firefly luciferase transcripts to the calculated FLUC/RLUC ratios in transfected cells, the RNA interference protocol targeting the bicistronic transcript could be conducted.

One other control experiment to discriminate the cryptic promoter activity originating from the inserted fragments in pRF vector system and the activity of putative IRESs is the RNA transfection approach. By introducing cells with *in vitro* transcribed mRNA instead of plasmid DNA, the cells will be devoid of the monocistronic firefly luciferase transcripts; thus, the contribution of cryptic promoters will become negligible [42]. Additionally, in various studies it is reported that cellular UTRs tend to generate cryptic transcripts [44–46]. Furthermore, it is previously stated that various UTRs are prone to cryptic splicing which eventually contributes to the firefly luciferase activity, thus; elevating the calculated FLUC/RLUC ratios [42]. Consequently, in order to eliminate these possibilities and conclude the presence of an IRES, further investi-

gations including RNAi knockdown approach [44] and RNA transfection strategy [42] could be employed for the IRES residing in the 5' UTR of KIM-1 mRNA.

In summary, we have tested the cytotoxic, proliferative, apoptotic and necrotic effects of OTA, CP and GM in HK-2 cell line and determined the optimum concentrations for treatment. Next, we have measured KIM-1 mRNA and protein levels under chemotoxic stress along with total protein synthesis. As we could not observe a reflection of the increase in KIM-1 protein levels in mRNA levels and global protein synthesis, we suspected existence of a post-transcriptional control mechanism. As the IRES usage under stress conditions is a common gene regulatory mechanism, we suspected that 5' UTR of KIM-1 mRNA might contain an IRES. Initially, we have identified the transcriptional start region using RLM-RACE experiments and defined the possible length of the KIM-1 mRNA's 5' UTR. Then, we tested our hypothesis by utilizing the bicistronic reporter assays. Indeed, we found an IRES that could function under chemotoxic stress where the rate of global translation is decreased drastically. Moreover, we have localized the minimal region of the 5' UTR that contains the functional IRES by deletional mutations. Nevertheless, further experimentation is needed in order to prove if this IRES is functional and responsive to the chemotoxic stress.

APPENDIX A: EQUIPMENT

Table A.1. Equipment.

4 °C **Room**	Birikim Elektrik, Turkey
Autoclaves	Astell Scientific, UK
Centrifuges	Beckman Coulter J2-MC superspeed centrifuge Du Pont, Combi, Sorvall Ultracentrifuge Eppendorf 5415C microcentrifuge
Electronic balance	Sartorius, Germany (TE412)
Electrophoresis Equipment	Bio-Rad Labs, USA (ReadySub-Cell GT Cells)
Fluorescence Microscope	Leica Microsystems, USA (MZ16FA)
Freezers	−20 °C Arçelik, Turkey −80 °C Thermo Electron Corp., USA
Gel documentation	Bio-Rad Labs, USA (GelDoc XR)
Confocal Microscope	Leica SP5-AOBS, USA
Vortex	Scientific Industries, USA
Sequencing	GenomeLab^{TM} GeXP Genetic Analysis System
Fluorescence Microscope	Leica Microsystems, USA (MZ16FA)
CO_2 Incubator	MCO-18AC, Sanyo, Japan
CO_2 Tank	Genç Karbon, Turkey
Dish Washer	Mielabor G7783, Miele, Germany
Laminar Flow Cabinet	Class II B, Tezsan, Turkey
Luminometer	Fluoroskan Ascent^{TM} FL, Thermo Scientific, USA

APPENDIX B: SUPPLIES

Table B.1. Cell culture chemicals and reagents.

Ochratoxin-A	Sigma-Aldrich, USA
Cisplatin	Santa Cruz, USA
Gentamicin	HyClone, USA
Dulbecco's Modified Eagle Medium (DMEM)	GibcoBRL, USA
Fetal Bovine Serum (FBS)	GibcoBRL, USA
0.25 % Trypsin/0.913 mM EDTA, Phenol Red	GibcoBRL, USA
Penicillin-Streptomycin Solution	GibcoBRL, USA
PBS	GibcoBRL, USA
RIPA	150 mM NaCl 1 % NP40 0.5 % Sodiumdeoxycolate 0.1% SDS 50 mM Tris pH 7.4
Protease Inhibitor Cocktail	Roche, Germany
Phosphatase Inhibitor Cocktail	Roche, Germany
Bovine Serum Albumin (BSA)	Thermo Scientific,USA
BCA Protein Assay Kit	Pierce, USA
XTT	Roche, Germany
CytoTox-Glo Cytotoxicity Assay	Promega, USA
NucleoBond Xtra Midi Kit	Macherey-Nagel, Germany

Table B.2. Western blotting solutions.

4X Protein Loading Dye	200mM TrisHCl pH 6.8 8% (w/v) SDS 40% (w/v) 100% Glycerol 4% (w/v) β-mercaptoethanol 50 mM EDTA 0.08% (w/v) Bromophenol Blue
12% Resolving gel	375 mM TrisHCl pH 8.8 0.1% (w/v) SDS Acrylamide:Bisacrylamide (12%/0.32% w/v) 0.05% (w/v) APS 0.005% (w/v) TEMED
Stacking Gel	0.125 mM TrisHCl pH 6.8 0.1% (w/v) SDS Acrylamide:Bisacrylamide (4%/0.1% w/v) 0.05% (w/v) APS 0.0075% (w/v) TEMED
Transfer Buffer	1% (w/v) Tris Base 14.4% (w/v) Glycine
TBS-T	50 mM TrisHCl pH 7.4 150 mM NaCl %0.05 Tween-20
Blocking Solution	5% (w/v) skim milk powder TBS-T
Primary Antibody Solution	5% (w/v)BSA 0.02% (w/v) Sodium Azide TBS-T
Secondary Antibody Solution	5% (w/v) skim milk TBS-T

REFERENCES

1. Bailly, V., Z. Zhang, W. Meier, R. Cate, M. Sanicola and J. Bonventre, "Shedding of Kidney Injury Molecule-1, a Putative Adhesion Protein Involved in Renal Regeneration", *Journal of Biological Chemistry*, Vol. 277, No. 42, pp. 39739–39748, 2002.

2. Ichimura, T., J. Bonventre, V. Bailly, H. Wei, C. Hession, R. Cate and M. Sanicola, "Kidney Injury Molecule-1 (KIM-1), a Putative Epithelial Cell Adhesion Molecule Containing a Novel Immunoglobulin Domain, is Upregulated in Renal Cells After Injury", *Journal of Biological Chemistry*, Vol. 273, No. 7, pp. 4135–4142, 1998.

3. Kaplan, G., A. Totsuka, P. Thompson, T. Akatsuka, Y. Moritsugu and S. Feinstone, "Identification of a Surface Glycoprotein on African Green Monkey Kidney Cells as a Receptor for Hepatitis A Virus.", *The European Molecular Biology Journal*, Vol. 15, No. 16, p. 4282, 1996.

4. Meyers, J., C. Sabatos, S. Chakravarti and V. Kuchroo, "The TIM-1 Gene Family Regulates Autoimmune and Allergic Diseases", *Trends in Molecular Medicine*, Vol. 11, No. 8, pp. 362–369, 2005.

5. Ichimura, T., E. Asseldonk, B. Humphreys, L. Gunaratnam, J. Duffield and J. Bonventre, "Kidney Injury Molecule–1 is a Phosphatidylserine Receptor That Confers a Phagocytic Phenotype on Epithelial Cells", *The Journal of Clinical Investigation*, Vol. 118, No. 5, p. 1657, 2008.

6. Schrier, R., W. Wang, B. Poole and A. Mitra, "Acute Renal Failure: Definitions, Diagnosis, Pathogenesis, and Therapy", *The Journal of Clinical Investigation*, Vol. 114, pp. 5–14, 2004.

7. Lim, A., S. Tang, K. Lai and J. Leung, "Kidney Injury Molecule-1: More Than Just an Injury Marker of Tubular Epithelial Cells?", *Journal of Cellular Physiology*,

2012.

8. Han, W. K., V. Bailly, R. Abichandani, R. Thadhani and J. V. Bonventre, "Kidney Injury Molecule-1 (KIM-1): a Novel Biomarker for Human Renal Proximal Tubule Injury", *Kidney International*, Vol. 62, No. 1, pp. 237–244, 2002.

9. Zhang, Z., B. D. Humphreys and J. V. Bonventre, "Shedding of the Urinary Biomarker Kidney Injury Molecule-1 (KIM-1) is Regulated by Map Kinases and Juxtamembrane Region", *Journal of the American Society of Nephrology*, Vol. 18, No. 10, pp. 2704–2714, 2007.

10. Vaidya, V., V. Ramirez, T. Ichimura, N. Bobadilla and J. Bonventre, "Urinary Kidney Injury Molecule-1: a Sensitive Quantitative Biomarker for Early Detection of Kidney Tubular Injury", *American Journal of Physiology-Renal Physiology*, Vol. 290, No. 2, pp. 517–529, 2006.

11. Han, W. K., A. Alinani, C.-L. Wu, D. Michaelson, M. Loda, F. J. McGovern, R. Thadhani and J. V. Bonventre, "Human Kidney Injury Molecule-1 is a Tissue and Urinary Tumor Marker of Renal Cell Carcinoma", *Journal of the American Society of Nephrology*, Vol. 16, No. 4, pp. 1126–1134, 2005.

12. Dieterle, F., E. Perentes, A. Cordier, D. R. Roth, P. Verdes, O. Grenet, S. Pantano, P. Moulin, D. Wahl and A. Mahl, "Urinary Clusterin, Cystatin C, Microglobulin and Total Protein as Markers to Detect Drug-Induced Kidney Injury", *Nature Biotechnology*, Vol. 28, No. 5, pp. 463–469, 2010.

13. Khandrika, L., S. Koul, R. B. Meacham and H. K. Koul, "Kidney Injury Molecule-1 is Upregulated in Renal Epithelial Cells in Response to Oxalate in Vitro and in Renal Tissues in Response to Hyperoxaluria in Vivo", *Plos One*, Vol. 7, No. 9, p. 44174, 2012.

14. Mukherjea, D., C. Whitworth, S. Nandish, G. Dunaway, L. Rybak and V. Ramkumar, "Expression of the Kidney Injury Molecule 1 in the Rat Cochlea and Induction

by Cisplatin", *Neuroscience*, Vol. 139, No. 2, pp. 733–740, 2006.

15. Ichimura, T., C. R. Brooks and J. V. Bonventre, "Kim-1/Tim-1 and Immune Cells: Shifting Sands", *Kidney International*, Vol. 81, No. 9, pp. 809–811, 2012.

16. Xiao, S., B. Zhu, H. Jin, C. Zhu, D. T. Umetsu, R. H. DeKruyff and V. K. Kuchroo, "Tim-1 Stimulation of Dendritic Cells Regulates the Balance Between Effector and Regulatory T Cells", *European Journal of Immunology*, Vol. 41, No. 6, pp. 1539–1549, 2011.

17. Rennert, P. D., "Novel Roles for TIM-1 in Immunity and Infection", *Immunology Letters*, Vol. 141, No. 1, pp. 28–35, 2011.

18. Arbillaga, L., A. Azqueta, O. Ezpeleta and A. L. de Cerain, "Oxidative Dna Damage Induced by Ochratoxin A in the Hk-2 Human Kidney Cell Line: Evidence of the Relationship With Cytotoxicity", *Mutagenesis*, Vol. 22, No. 1, pp. 35–42, 2006.

19. Walker, R., "Risk Assessment of Ochratoxin: Current Views of the European Scientific Committee on Food, the JECFA and the Codex Committee on Food Additives and Contaminants", *Mycotoxins and Food Safety*, pp. 249–255, Springer, 2002.

20. de Groene, E. M., A. Jahn, G. J. Horbach and J. Fink-Gremmels, "Mutagenicity and Genotoxicity of the Mycotoxin Ochratoxin A", *Environmental Toxicology and Pharmacology*, Vol. 1, No. 1, pp. 21–26, 1996.

21. Wagacha, J. and J. Muthomi, "Mycotoxin Problem in Africa: Current Status, Implications to Food Safety and Health and Possible Management Strategies", *International Journal of Food Microbiology*, Vol. 124, No. 1, pp. 1–12, 2008.

22. Creppy, E., A. Kane, G. Dirheimer, C. Lafarge-Frayssinet, S. Mousset and C. Frayssinet, "Genotoxicity of Ochratoxin A in Mice: DNA Single-Strand Break Evaluation in Spleen, Liver and Kidney", *Toxicology Letters*, Vol. 28, No. 1, pp. 29–35, 1985.

23. Gillman, I. G., T. N. Clark and R. A. Manderville, "Oxidation of Ochratoxin A by an Feporphyrin System: Model for Enzymatic Activation and Dna Cleavage", *Chemical Research in Toxicology*, Vol. 12, No. 11, pp. 1066–1076, 1999.

24. Božić, Z., V. Duančić, M. Belicza, O. Kraus and I. Skljarov, "Balkan Endemic Nephropathy: Still a Mysterious Disease", *European Journal of Epidemiology*, Vol. 11, No. 2, pp. 235–238, 1995.

25. Sundin, D. P., R. Sandoval and B. A. Molitoris, "Gentamicin Inhibits Renal Protein and Phospholipid Metabolism in Rats: Implications Involving Intracellular Trafficking", *Journal of the American Society of Nephrology*, Vol. 12, No. 1, pp. 114–123, 2001.

26. Turnidge, J., "Pharmacodynamics and Dosing of Aminoglycosides", *Infectious Disease Clinics of North America*, Vol. 17, No. 3, pp. 503–528, 2003.

27. Moulds, R. F. and M. S. Jeyasingham, "Gentamicin: A Great Way to Start", *Australian Prescriber*, Vol. 33, No. 5, pp. 134–135, 2010.

28. Lopez-Novoa, J. M., Y. Quiros, L. Vicente, A. I. Morales and F. J. Lopez-Hernandez, "New Insights Into the Mechanism of Aminoglycoside Nephrotoxicity: An Integrative Point of View", *Kidney International*, Vol. 79, No. 1, pp. 33–45, 2010.

29. Beauchamp, D., G. Laurent, P. Maldague, S. Abid, B. Kishore and P. M. Tulkens, "Protection Against Gentamicin Induced Early Renal Alterations (Phospholipidosis and Increased Dna Synthesis) by Coadministration of Poly-L-aspartic Acid.", *Journal of Pharmacology and Experimental Therapeutics*, Vol. 255, No. 2, pp. 858–866, 1990.

30. Trzaska, S., "Cisplatin", *Chemical and Engineering News*, Vol. 83, No. 25, pp. 52–52, 2005.

31. Arany, I. and R. L. Safirstein, "Cisplatin Nephrotoxicity", *Seminars in Nephrology*, Vol. 23, pp. 460–464, 2003.

32. Kröning, R., A. Lichtenstein and G. Nagami, "Sulfur Containing Amino Acids Decrease Cisplatin Cytotoxicity and Uptake in Renal Tubule Epithelial Cellines", *Cancer Chemotherapy and Pharmacology*, Vol. 45, No. 1, pp. 43–49, 2000.

33. Arany, I., J. K. Megyesi, H. Kaneto, P. M. Price and R. L. Safirstein, "Cisplatin Induced Cell Death is EGFR/src/ERK Signaling Dependent in Mouse Proximal Tubule Cells", *American Journal of Physiology-Renal Physiology*, Vol. 287, No. 3, pp. 543–549, 2004.

34. Amin, R. P., A. E. Vickers, F. Sistare, K. L. Thompson, R. J. Roman, J. Lawton, H. K. Hamadeh, J. Collins and S. Grissom, "Identification of Putative Gene Based Markers of Renal Toxicity", *Environmental Health Perspectives*, Vol. 112, No. 4, p. 465, 2004.

35. Holcik, M. and N. Sonenberg, "Translational Control in Stress and Apoptosis", *Nature Reviews Molecular Cell Biology*, Vol. 6, No. 4, pp. 318–327, 2005.

36. Jackson, R. J., C. U. Hellen and T. V. Pestova, "The Mechanism of Eukaryotic Translation Initiation and Principles of Its Regulation", *Nature Reviews Molecular Cell Biology*, Vol. 11, No. 2, pp. 113–127, 2010.

37. Spriggs, K. A., L. C. Cobbold, S. H. Ridley, M. Coldwell, A. Bottley, M. Bushell, A. E. Willis and K. Siddle, "The Human Insulin Receptor Mrna Contains a Functional Internal Ribosome Entry Segment", *Nucleic Acids Research*, Vol. 37, No. 17, pp. 5881–5893, 2009.

38. Pain, V. M., "Initiation of Protein Synthesis In Eukaryotic Cells", *European Journal of Biochemistry*, Vol. 236, No. 3, pp. 747–771, 1996.

39. Yaman, I., J. Fernandez, H. Liu, M. Caprara, A. A. Komar, A. E. Koromilas,

L. Zhou, M. D. Snider, D. Scheuner and R. J. Kaufman, "The Zipper Model of Translational Control: A Small Upstream ORF is the Switch That Controls Structural Remodeling of An Mrna Leader", *Cell*, Vol. 113, No. 4, pp. 519–531, 2003.

40. Spriggs, K. A., M. Bushell and A. E. Willis, "Translational Regulation of Gene Expression During Conditions of Cell Stress", *Molecular Cell*, Vol. 40, No. 2, pp. 228–237, 2010.

41. Il'ichev, Y. V., J. L. Perry and J. D. Simon, "Interaction of Ochratoxin A with Human Serum Albumin. Preferential Binding of the Dianion and Ph Effects", *The Journal of Physical Chemistry B*, Vol. 106, No. 2, pp. 452–459, 2002.

42. Bert, A. G., R. Grépin, M. A. Vadas and G. J. Goodall, "Assessing Ires Activity in the HIF-1α and Other Cellular 5$'$ UTRs", *Rna*, Vol. 12, No. 6, pp. 1074–1083, 2006.

43. Vopálenskỳ, V., T. Mašek, O. Horváth, B. Vicenová, M. Mokrejš and M. Pospíšek, "Firefly Luciferase Gene Contains a Cryptic Promoter", *Rna*, Vol. 14, No. 9, pp. 1720–1729, 2008.

44. Van Eden, M. E., M. P. Byrd, K. W. Sherill and R. E. Lloyd, "Demonstrating Internal Ribosome Entry Sites in Eukaryotic Mrnas Using Stringent Rna Test Procedures", *Rna*, Vol. 10, No. 4, pp. 720–730, 2004.

45. Han, B. and J.-T. Zhang, "Regulation of Gene Expression by Internal Ribosome Entry Sites or Cryptic Promoters: The Eif4g Story", *Molecular and Cellular Biology*, Vol. 22, No. 21, pp. 7372–7384, 2002.

46. Sherrill, K. W., M. P. Byrd, M. E. Van Eden and R. E. Lloyd, "BCL-2 Translation is Mediated Via Internal Ribosome Entry During Cell Stress", *Journal of Biological Chemistry*, Vol. 279, No. 28, pp. 29066–29074, 2004.

47. Tsukiyama-Kohara, K., N. Iizuka, M. Kohara and A. Nomoto, "Internal Ribosome Entry Site Within Hepatitis C Virus Rna", *Journal of Virology*, Vol. 66, No. 3, pp. 1476–1483, 1992.

48. Ghattas, I. R., J. Sanes and J. Majors, "The Encephalomyocarditis Virus Internal Ribosome Entry Site Allows Efficient Coexpression of Two Genes From a Recombinant Provirus in Cultured Cells and In Embryos", *Molecular and Cellular Biology*, Vol. 11, No. 12, pp. 5848–5859, 1991.

49. Komar, A. A. and M. Hatzoglou, "Internal Ribosome Entry Sites in Cellular Mrnas: Mystery of Their Existence", *Journal of Biological Chemistry*, Vol. 280, No. 25, pp. 23425–23428, 2005.

50. Fernandez, J., I. Yaman, R. Mishra, W. C. Merrick, M. D. Snider, W. H. Lamers and M. Hatzoglou, "Internal Ribosome Entry Site-Mediated Translation of A Mammalian Mrna is Regulated by Amino Acid Availability", *Journal of Biological Chemistry*, Vol. 276, No. 15, pp. 12285–12291, 2001.

51. Fernandez, J., I. Yaman, W. C. Merrick, A. Koromilas, R. Wek, J. Hensold and M. Hatzoglou, "Regulation of Ires Mediated Translation by Eukaryotic Initiation Factor-2α Phosphorylation and Translation of a Small Upstream Open Reading Frame", *Journal of Biological Chemistry*, Vol. 277, No. 3, pp. 2050–2058, 2002.

52. Hellen, C. U. and P. Sarnow, "Internal Ribosome Entry Sites in Eukaryotic Mrna Molecules", *Genes and Development*, Vol. 15, No. 13, pp. 1593–1612, 2001.

53. Kozak, M., "Structural Features in Eukaryotic Mrnas That Modulate the Initiation of Translation", *Journal of Biological Chemistry*, Vol. 266, No. 30, pp. 19867–19870, 1991.

54. Schmidt, E. K., G. Clavarino, M. Ceppi and P. Pierre, "Sunset, a Nonradioactive Method to Monitor Protein Synthesis", *Nature Methods*, Vol. 6, No. 4, pp. 275–277, 2009.

55. Brivet, F. G., D. J. Kleinknecht, P. Loirat and P. J. Landais, "Acute renal failure in intensive care units–causes, outcome, and prognostic factors of hospital mortality: a prospective, multicenter study", *Critical care medicine*, Vol. 24, No. 2, pp. 192–198, 1996.

56. Bellomo, R., C. Ronco, J. A. Kellum, R. L. Mehta, P. Palevsky *et al.*, "Acute renal failure–definition, outcome measures, animal models, fluid therapy and information technology needs: the Second International Consensus Conference of the Acute Dialysis Quality Initiative (ADQI) Group", *Critical care*, Vol. 8, No. 4, p. R204, 2004.

57. Lock, E. A., "Sensitive and early markers of renal injury: where are we and what is the way forward?", *Toxicological sciences*, Vol. 116, No. 1, pp. 1–4, 2010.

58. Thadhani, R., M. Pascual and J. V. Bonventre, "Acute Renal Failure", *New England Journal of Medicine*, Vol. 334, No. 22, pp. 1448–1460, 1996.

59. Mehta, R. L., J. A. Kellum, S. V. Shah, B. A. Molitoris, C. Ronco, D. G. Warnock and A. Levin, "Acute Kidney Injury Network: Report of an Initiative to Improve Outcomes in Acute Kidney Injury", *Critical Care*, Vol. 11, No. 2, p. R31, 2007.

60. Uchino, S., J. A. Kellum, R. Bellomo, G. S. Doig, H. Morimatsu, S. Morgera, M. Schetz, I. Tan, C. Bouman and E. Macedo, "Acute Renal Failure in Critically Ill Patients: A Multinational, Multicenter Study", *Jama*, Vol. 294, No. 7, pp. 813–818, 2005.